Università di Pisa

Dottorato di Ricerca
Tecnologie per la salute: valutazione e gestione delle innovazioni nel settore biomedicale

IMAGING DI FUSIONE E NUOVE TECNOLOGIE ABLATIVE IN ONCOLOGIA INTERVENTISTICA

Presidente:
Prof. Andrea Pietrabissa

Tutor:
Prof. Riccardo Lencioni

Candidato:
Dr.ssa Laura Crocetti

Anno Accademico 2005/2006

INDEX

RESEARCH PROJECT

Tumor ablation by means of other than traditional surgical approaches is a methodology attempted with modest success for a number of years. During the past few years however, the use of image-guided interventions in cancer treatment has experienced unparalleled growth. Modern approaches take advantage of the vastly superior armamentarium of imaging strategies now available. Advances in material science, and methods for delivery of ablating agents combined with improved localization now make possible to be much more aggressive and effective in attempting to achieve local ablation of malignant tumors. Interventional Oncology is gaining increasing acceptance as a viable alternate or complementary treatment for a variety of cancers.

Ongoing research in industry and academic centers is focused on two clinical needs: to overcome limitations of current imaging modalities in guiding and monitoring ablation procedures and to produce larger zones of ablation in different organs in a safe and reproducible fashion.

Ultrasound (US) is considered as imaging modality of choice for guiding percutaneous ablation procedures in the liver, with computed tomography (CT) guidance being reserved for lesions inconspicuous on US. However, there are occasions when the liver lesion is only optimally visualized on contrast-enhanced CT and magnetic resonance (MR) imaging, making targeting and monitoring difficult, due to lack of real-time imaging guidance. Given the advantages of US guidance, it would be ideal if the procedure can be performed with real-time US matched with supplementary information from contrast enhanced CT or MR images. Fusion imaging, the process of aligning and superimposing images obtained using two different imaging modalities, is a rapidly evolving field of interest, with its own specific operational conditions. The Phase I of this Research Project was designed to investigate the feasibility and validity of real-time guidance using a virtual navigation system that fused US and CT information in

targeting and ablating, by means of radiofrequency, a liver target inconspicuous on US.

Phases II and III were designed to assess feasibility and safety of new ablative technologies in lung ablation in experimental animal models. In Phase II multitined perfused electrode needles were used to perform radiofrequency ablation of rabbit lung tissue. The potential benefits of using saline-enhanced RF ablation could be important in lung ablation, because of the tissue characteristics of the lung. In fact, air containing lung tissue has a naturally high tissue impedance, and this makes difficult to create a safety margin around the treated lesion . On the other hand, direct and uncontrollable thermal damage to adjacent and remote structures was observed more frequently using saline infusion during RF ablation than conventional RF ablation. The aims of Phase II were therefore to assess feasibility and safety of RF ablation of lung tissue performed with multitined perfused electrodes.

Together with new RF devices, also alternative sources of energy are under investigation to overcome conventional RF ablation limits. With several theoretic and practical advantages, microwave (MW) ablation is a promising new option in the treatment of surgically unresectable tumors. The potential benefits of MW technology include consistently higher intratumoral temperatures, larger tumor ablation volumes, faster ablation times, improved convection profile and less procedural pain. Phase III was designed to know how MW ablation affects normal lung tissue, comparing a prototype MW ablation system with a commercially available RF device in an in-vivo lung rabbit model.

LIVER LESIONS TARGETING AND ABLATION WITH A FUSION IMAGING SYSTEM: AN EXPERIMENTAL FEASIBILITY STUDY

ABSTRACT

Purpose: To investigate the feasibility and validity of real-time guidance using a fusion imaging system that combined ultrasound (US) and computed tomography (CT) in the targeting and subsequent radiofrequency (RF) ablation of a liver target inconspicuous on US.

Methods and Materials: The study was designed as an experimental ex-vivo study in calf livers with radiopaque internal targets, inconspicuous at US, simulating a focal liver lesion. The study included two phases. The initial phase was to examine the feasibility of matching pre-procedural volumetric CT data of the calf livers with real-time US using a commercially available multimodality fusion imaging system (Virtual Navigator System, Esaote SpA, Genoa, Italy), and to assess the accuracy of targeting using a 22 gauge (G) cytological needle using the system. The second phase of the study was to validate such a technique using a 15G RF multitined expandable needle (RITA Medical Systems, Mountain View, CA) and to examine the accuracy of the needle placement relative to the target. Unenhanced CT of the liver and multiplanar reconstructions were performed to calculate respectively the distance between the needle and the pellet and the distance between the central tine of the RF electrode and the pellet.

Results: All calf livers underwent successful CT-US registration with a mean registration error of 0.30 ± 0.01 cm and 0.29 ± 0.01 cm in the initial and second phase of the study, respectively. In the initial phase an overall number of 24 insertions were performed following the US-CT guidance. The needle to target distance was 1.9 ± 0.7 mm (range 0.84-3 mm). In the second phase an overall number of 12 ablations were performed and only one insertion was done to place the electrode following the US-CT guidance. The mean target-central tine

distance, recorded at post-procedural CT, was 3.9 ± 0.7 mm (range 2.94-5.14 mm).After the dissection of the specimen the pellet was found unchanged in the center of the ablation zone in all cases

Conclusion: Real-time registration and fusion of pre-procedure CT volume images with intra-procedure US is feasible and accurate. For lesion hardly visible at US or CT or for more complex procedures, such as thermal tumor ablations that require positioning of multiple applicators and puncture of multiple lesions, navigation systems might be of help to reduce puncture risk and procedure time and to allow for more complete and radical therapy.

INTRODUCTION

Image guidance is essential in the treatment of liver tumors using percutaneous ablative techniques. Apart from careful pre-procedure planning and elaborate post-procedure evaluation, accurate intra-procedure targeting, monitoring, and controlling play a critical role in the success of the technique [1].

In our centre radiofrequency (RF) ablation is most commonly performed under ultrasound (US) guidance, with computed tomography (CT) guidance being reserved for lesions inconspicuous on US. However, there are occasions when the liver lesion is only optimally visualized on contrast-enhanced CT and magnetic resonance (MR) imaging, making targeting and monitoring difficult due to lack of real-time imaging guidance. In this scenario, it would be desirable to fuse information from different imaging modalities (e.g., US and CT) and such multimodality matching have been utilized in nuclear medicine, radiotherapy, and neurosurgery [2-4] .

In this study, we investigate the feasibility and validity of real-time guidance using a fusion imaging system that combined US and CT information in the targeting and subsequent RF ablation of a liver target inconspicuous on US.

MATERIALS AND METHODS

Study Design

The study was designed as an experimental ex-vivo study in calf livers with radiopaque internal targets simulating a focal liver lesion. The approval by local Research Ethics Committee was obtained. The study included two phases. The initial phase was to examine the feasibility of matching pre-procedural volumetric CT data of the calf livers with real-time US using a commercially available multimodality fusion imaging system (Virtual Navigator System, Esaote SpA, Genoa, Italy), and to assess the accuracy of targeting using a 22 gauge (G) cytological needle using the system. The second phase of the study was to validate such a technique using a 15G RF multitined expandable needle and to examine the accuracy of the needle placement relative to the target.

Target

Radiopaque targets were represented by 1.5mm lead pellets, inconspicuous on conventional US but with high attenuation on CT. They allow realistic puncture by either of the needle types employed in our study. The pellet was implanted into calf liver, by using an 11 G soft introducer, 13 cm in length (StarBurst Soft Tissue Access System, RITA Medical System, Mountain View, CA). Soft introducers can be used with multitined expandable electrode needles, for the coagulation and ablation of soft tissue. They have a flexible sheath with a tapered tip and a blunt edge and a stainless steel stylet with three-face trocar point for cutting and dilation of tissue. In this study we used these introducers to place the bullets inside the calf liver. The introducer was inserted into the liver parenchyma from lateral liver side, to avoid the disruption of superior liver surface. After removing the stainless steel stylet, the pellet was put into the sheath and pushed inside the liver by means of the stylet. In each calf liver 4 pellets were inserted.

Fusion Imaging System

The system consists of an US scanner connected to the Navigation unit. The two units are connected by a video cable to grab the ultrasound screen and a network cable to query the current scan geometry of the US scanner. An electromagnetic tracking system, composed by a transmitter and a small receiver (mounted on the US probe) provides the position and orientation of the US probe in relation to the transmitter. This permits a correct representation in size and orientation of the second modality image. These data are provided by the US scanner by the network connection and automatically updated at every change on the console of the Navigation unit. The system specifications are provided in Tab.1.

The electromagnetic tracker is sensitive to metallic objects close or near the receiver or transmitter. Thus, any metallic material that may interfere and disturb the magnetic field must be avoided between the transmitter and the receiver.

Fusion Imaging System Setup

Prior to the intervention a four-step protocol was followed:

1. Ten 1.5mm radio-opaque fiducial markers (X-Spots, Beekley, Bristol, CT) were applied to the calf liver capsule, in order to correlate (register) the CT scan with the US scan.
2. Pre-procedure unenhanced multidetector CT (MDCT) of the liver was then performed using a 4-row scanner (LightSpeed Plus CT ,GE Medical Systems, Milwaukee, Wis) with a 1.25 mm collimation and a reconstruction interval of 0.6 mm, covering the external markers.
3. The CT DICOM series were transferred to the Virtual Navigator System by using the Picture Archiving and Communicating System (PACS).
4. The navigation system is coupled with an US machine (Technos MPX; Esaote, Genoa, Italy) and registration of the position of each fiducial marker to the system was executed in 2 stages. First the positions of all the

fiducial markers in the CT volume were identified and numbered (Figure 1a). Secondly the corresponding positions on the cow livers were matched by applying point contact with a registration pin (Figure 1b) from the system on each marker. The sequence was in accordance with the number given during the first stage. Accuracy or error of registration will be displayed by the system following completion of registration of all the 10 positions (Figure 1c).

Real-time US of the calf livers was then performed using a 3.5Hz curvilinear probe with the images being displayed on the monitor of the Virtual Navigator System, next to the corresponding CT volumetric images. A sterilizable biopsy kit for convex array (ABS 421, Esaote, Genoa, Italy), with a biopsy needle angle of 20° was used to guide the needle insertion. The US images could also be reverted to CT images on the same screen. Accuracy of the matched US-CT images was also subjectively assessed by the operator, using specific anatomical markers (i.e. air within liver vessels)

Phase I: Targeting

This was performed in 3 calf livers. The target was identified on the 'real-time' CT images during US assessment. As it was inconspicuous on US, the target was marked on the CT image and the corresponding location was pointed out by the system on the US image. The optimal biopsy route was chosen and a biopsy track was visualized (Fig. 2).

A 21 G cytological needle 20 cm in length (Quinjekt, Hospital Service, Roma, Italy) was advanced into the liver parenchyma under real-time ultrasound visualization, with the attached biopsy kit (Fig. 3). The tip of the needle should ideally be placed in the target, but given the small dimensions and the solid nature of it, we considered to go the nearest as possible to the pellet. Two targeting procedures were performed per pellet, by two radiologists experienced in CT- and

US-guided percutaneous interventions. Only one needle pass had to be performed for each targeting procedure. The accuracy of targeting was assessed on a repeat CT examination with the needles in-situ. Unenhanced MDCT of the liver was performed with a 1.25 mm collimation and a reconstruction interval of 0.6 mm, covering the entire liver. The distance between the needle and the pellet was calculated on multiplanar reconstructed CT images (reconstruction interval of 1 mm), along a plane perpendicular to the needle.

Phase II: Radiofrequency ablation of the target

RF ablation was performed in 3 calf livers. Target localization was performed and a 15 G RF multitined expandable electrode needle (Starburst XL, RITA Medical Systems, Mountain View, CA) was inserted into the liver using real-time guidance and biopsy kit, considering the target as the ideal centre of the ablation. The tip of the trocar was placed 1 cm from the centre of the intended ablation area (i.e. the pellet) for a 3 cm ablation, according to the manufacturer recommendations (Fig. 4). Following deployment of the tines to 3 cm, RF ablation was performed with a 200-W generator (model 1500; RITA Medical System, Mountain View, CA) at target temperature of 95 °C for 15 minutes. Continuous real-time US monitoring was performed during RF ablation. The target is heat resistant and therefore remained intact allowing visualization on a repeat CT post procedure. Only one needle pass had to be performed for each ablation procedure. Following ablation, the accuracy of targeting was assessed on a repeat CT examination with the needles in-situ. Unenhanced MDCT of the liver was performed with a 1.25 mm collimation and a reconstruction interval of 0.6 mm, covering the entire liver. The distance between the central tine and the pellet was calculated on multiplanar reconstructed CT images (reconstruction interval of 1 mm), along a plane perpendicular to the electrode. The liver was then cut along the electrode axis and the accuracy of RF targeting was assessed.

Results analysis

Registration error due to matching misalignment is expressed in cm by the navigation system. Results are expressed as mean ± SD for continuous data. Target accuracy is defined as the distances in mm between the epicentre of the target and the Chiba needle in the first phase of the study, and the distances in mm between the epicentres of the target and the tip of the central tine of the multitined RF electrode needle in the second phase.

RESULTS

All calf livers underwent successful CT-US registration with a mean registration error of 0.30 ± 0.01 cm and 0.29 ± 0.01 cm in the initial and second phase of the study, respectively.

After some experience in setting up the navigation system we were able to perform the system setup including the registration within 3-5 min.

In phase I each pellet was used for two US-CT guided targeting insertions. An overall number of 24 insertions were performed with the aim of placing the Chiba needle the nearest as possible to the pellet, following the US-CT guidance. The needle to target distance was 1.9 ± 0.7 mm (range 0.84-3 mm) (Fig. 5).

In phase II each pellet was used for one US-CT guided ablation. An overall number of 12 ablations were performed and only one insertion was done to place the electrode 1 cm from pellet, following the US-CT guidance. The mean target-central tine distance, recorded at post-procedural CT, was 3.9 ± 0.7 mm (range 2.94-5.14 mm).

After the dissection of the specimen the pellet was found unchanged in the center of the ablation zone in all cases (Fig.6).

Table 1. System specifications

Module	Description
US Scanner	Technos ^{MPX} Esaote S.p.A
US Probe	Convex array 6-2 MHz
Network connection	TCP/IP protocol
Navigation Unit	Virtual Navigator Esaote S.pA
Tracking system	PCIBirds (ASCENSION TECNOLOGY) Degrees of freedom: Six (position and orientation) Translation range, any direction: Standard transmitter = +/- 30 (76.2 cm) Angular range: All attitude Static accuracy standard sensor: .040 (1.0 mm) RMS position 0.15 degree RMS orientation

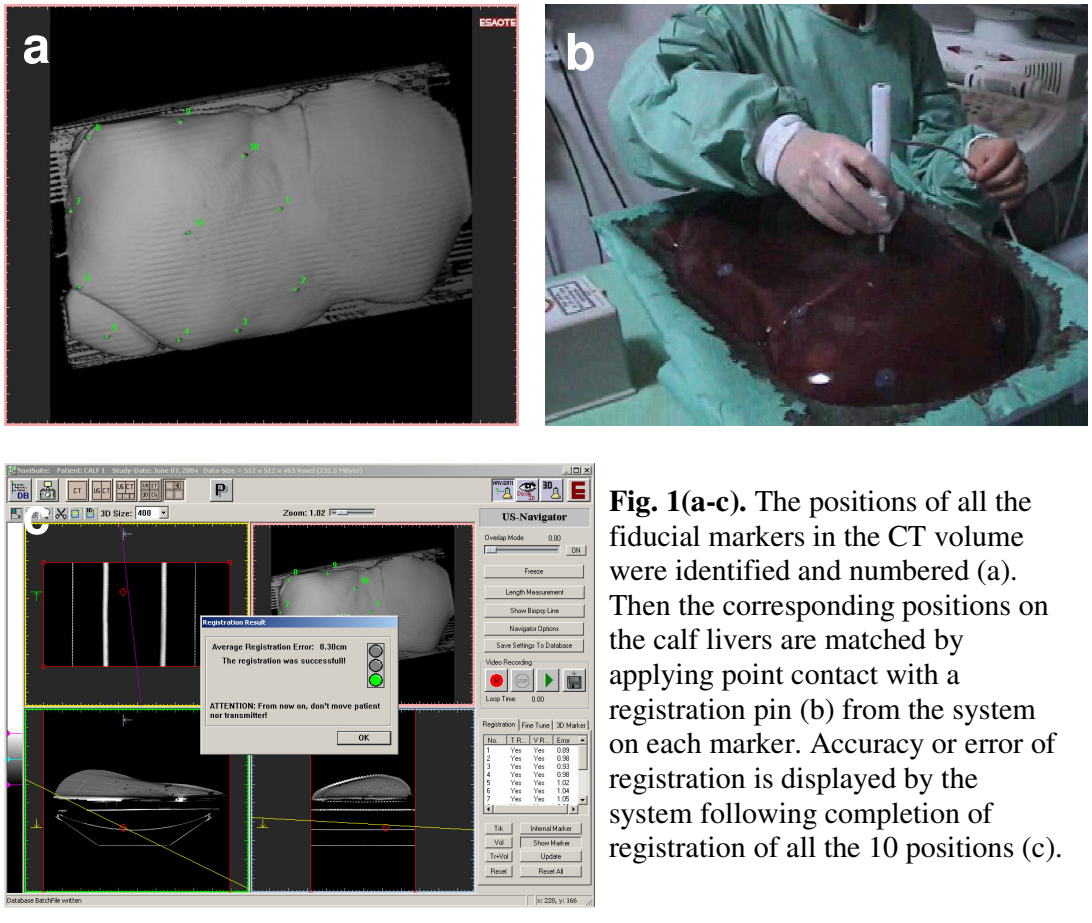

Fig. 1(a-c). The positions of all the fiducial markers in the CT volume were identified and numbered (a). Then the corresponding positions on the calf livers are matched by applying point contact with a registration pin (b) from the system on each marker. Accuracy or error of registration is displayed by the system following completion of registration of all the 10 positions (c).

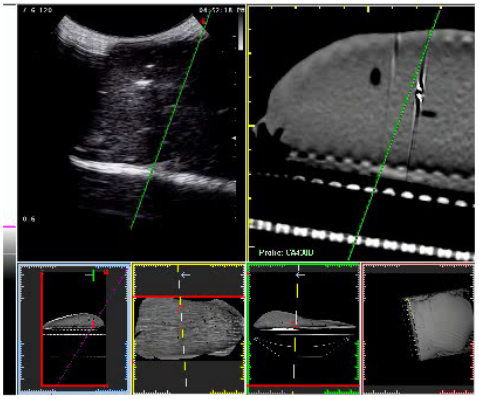

Fig.2

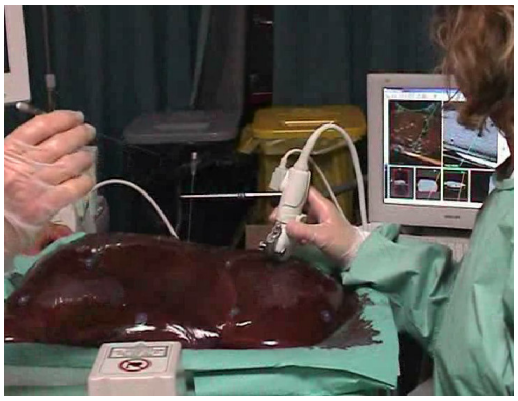

Fig.3

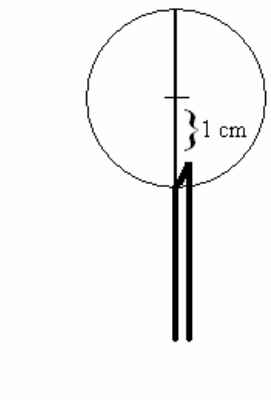

Fig.4

Fig. 2. The target is identified on the 'real-time' CT images during US assessment. The optimal biopsy route was chosen and a biopsy track was visualized.
Fig.3. A 21 G cytological needle 20 cm in length is used, together with the attached biopsy kit. In the back the matched US-CT image on the Virtual Navigator screen.
Fig.4. The tip of the trocar has to placed 1 cm from the centre of the intended ablation area (i.e. the pellet) for a 3 cm
Fig.5 (a,b). Multiplanar reconstructed CT images showing the distance between the pellet and the needle that was inserted under US-CT guidance

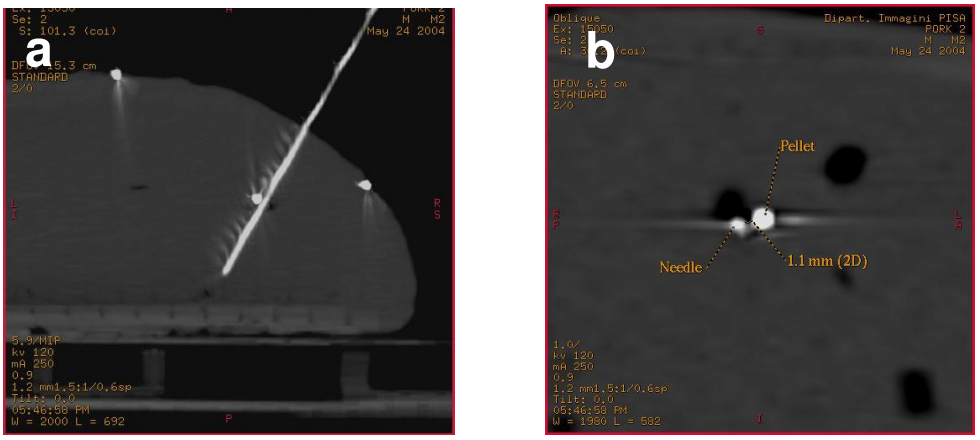

Fig 5 (a,b)

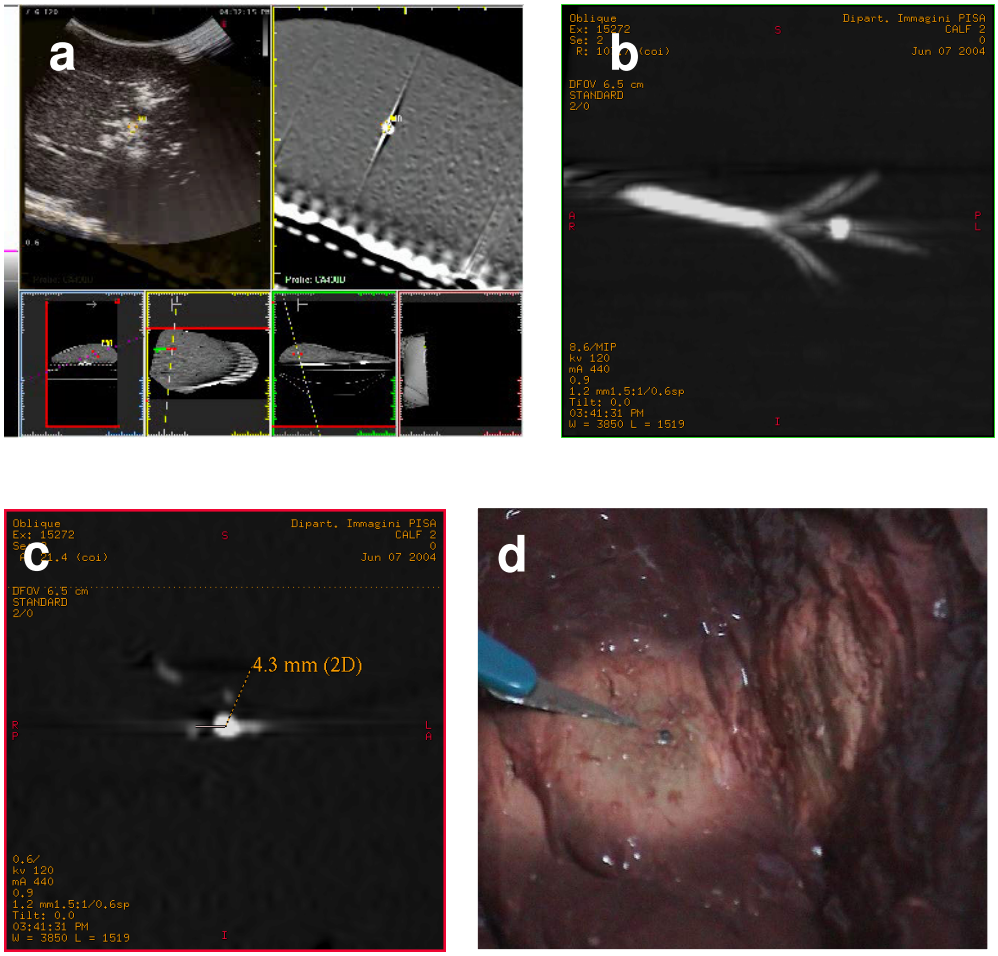

Fig. 6 (a-d). The target is identified on the 'real-time' CT images during US assessment and a 15 G RF multitined expandable electrode is inserted into the liver considering the target as the ideal centre of the ablation (a). Multiplanar reconstructed CT images show the relationship between the deployed hooks and the pellet (b) and the distance between the central tine and the pellet is calculated along a plane perpendicular to the electrode (c). After the dissection of the specimen the pellet is found unchanged in the center of the ablation zone (d)

DISCUSSION

US is a widely used tool for imaging guided procedures in the abdomen, especially in the liver. US is fast, easily available, allows real time imaging and is characterized by high natural contrast among parenchyma, lesions, and vessels. On the other hand, because of its high spatial resolution, good contrast, wide field of view, good reproducibility, and applicability to bony and air-filled structures, CT plays an important role especially in interventions which cannot be adequately guided by fluoroscopy or US [5-7]. However, in contrast to fluoroscopy and US, CT has been limited by the lack of real-time imaging so that many CT-guided abdominal interventions remain difficult or risky in several locations [8]. Moreover, the contrast resolution of baseline CT scan is low and many liver lesions are visible only during arterial and/or portal-venous phase of the dynamic study and not uncommonly needle localization under un-enhanced phase of image guidance is based on nearby anatomical landmarks [9]. The introduction of CT fluoroscopy allows real-time display of CT images with a markedly decreased patient radiation dose and total procedure time comparable with the use of conventional CT guidance [10]. Moreover new systems of breath-hold monitoring have been implemented and this could allow an easier access to mobile lesions [11]. However, despite marked improvements in procedure times compared with helical CT, CT fluoroscopy may still require 40% longer procedure times than US [12].

Therefore the ideal qualities of a targeting technique during image-guided liver procedures include clear delineation of the tumour(s) and the surrounding anatomy, coupled with real-time imaging and multiplanar and interactive capabilities [1]. Given the advantage of US guidance, it would be ideal if the procedure can be performed with real-time US matched with supplementary information from contrast enhanced CT or MR images. Numerous devices have been constructed to improve puncture accuracy for percutaneous radiological interventions and majority of these are based on CT [13-17]. Image fusion, the

process of aligning and superimposing images obtained using two different imaging modalities, is a rapidly evolving field of interest, with its own specific operational conditions [18-20].

To our knowledge this is the first report concerning the accuracy of targeting by using an image fusion system that matches real-time US and CT. In our feasibility study, we demonstrated a high and consistent level of matching accuracy with mean registration error 0.30 ± 0.01 cm and 0.29 ± 0.01 cm in the initial and second phase of the study, respectively. Apart from external markers, registration of CT data to intra-procedure US images using specific anatomical (e.g., portal and hepatic veins) and topographical (xiphoid sternum and umbilicus) landmarks can also be accomplished in real-time during US examination. For anatomical matching, accuracy in defining the specific point pairs in both CT and US images is necessary to obtain the best registration results.

We used a target that was undetectable at US and that was very small in size (1.5 mm). This ideally represents the situation of a tiny lesion that is visible only at CT. The navigation system represented therefore the only guidance for the procedures. By deciding to insert the needle only once for each targeting/ablation procedure, we reproduced the need of minimal invasiveness.

Excellent target accuracy was achieved in both phases of the study, with an acceptable mean needle to target distance of 1.9 ± 0.7 mm (range 0.84-3 mm) in phase I and a mean target-central tine distance of 3.9 ± 0.7 mm (range 2.94-5.14 mm) in phase II. Two our knowledge this is the first report about the accuracy of a fusion imaging system combining real time US with pre-acquired CT.

The main limitation of the study is the absence respiratory excursion and subject motion in this ex-vivo model. Either or both of these factors would introduce error but were not evaluated in our feasibility study. To extrapolate the utility in routine clinical practice, precise registration of CT volume images into the patient requires proper synchronisation with respect to the respiratory phase and arms' position during CT examination, and patient movement must be avoided. We appreciate that added procedure time may be required to achieve

accurate patient registration in some cases, but this may be offset by the time taken to perform needle localization and RF ablation of a lesion invisible or poorly conspicuous on routine unenhanced US or CT. Possible solutions for detection of patient movement would be the implementation of external electromagnetic position sensors to the patient's body. To target liver lesions that move during the breathing cycle, a breathing motion correction must be implemented. The solution could be based on methods used in radiation therapy, as well as on those used in positron emission tomography–CT image fusion [21-22].

Future advances include the automation of registration, which could further streamline clinical translation of such technologies. Miniaturization of internalized sensors for electromagnetic tracking of needles and ablation probes will have the ability to transform image guided needle-based procedures by providing real-time multi-modality feedback.

In conclusion real-time registration and fusion of pre-procedure CT volume images with intra-procedure US is feasible and accurate. For simple biopsies, an experienced interventionalist will not ask for such a guidance tool and, given the cost and availability, US and CT guidance will remain the "workhorses" for biopsy procedures. For lesion hardly visible at US or CT or for more complex procedures, such as thermal tumor ablations that require positioning of multiple applicators and puncture of multiple lesions, fusion imaging systems might be of help to reduce puncture risk and procedure time and to allow for more complete and radical therapy.

REFERENCES

1. Goldberg SN, Grassi CJ, Cardella JF, et al (2005) Image-guided tumour ablation: Standardization of terminology and reporting criteria. JVIR 16:765-778
2. Tsukamoto E, Ochi S (2006) PET/CT today: system and its impact on cancer diagnosis. Ann Nucl Med 20:255-267
3. Ma CM, Paskalev K (2006) In-room CT techniques for image-guided radiation therapy. Med Dosim 31:30-39
4. Grunert P, Darabi K, Espinosa J, Filippi R (2003) Computer-aided navigation in neurosurgery. Neurosurg Rev 26:73-99
5. Haaga JR, Reich NE, Havrilla TR, et al(1977) Interventional CT scanning. Radiol Clin North Am 15:449–456
6. Sheafor DH, Paulson EK, Simmons CM, DeLong DM, Nelson RC (1998) Abdominal percutaneous interventional procedures: comparison of CT and US guidance. Radiology 207:705-710
7. Kliewer MA, Sheafor DS, Paulson EK, Helsper RS, Hertzberg BS, Nelson RC (1999) Percutaneous liver biopsy: a cost benefit analysis comparing sonographic and CT guidance. AJR173:1199-1202
8. Daly B, Templeton PA (1999) Real-time CT fluoroscopy: evolution of an interventional tool. Radiology 211:309–331
9. Lencioni R, Cioni D, Bartolozzi C (2005) Focal Liver Lesions. Springer-Verlag, Berlin Heidelberg New York
10. Carlson SK, Bender CE, Classic KL, et al (2001) Benefits and safety of CT fluoroscopy in interventional radiologic procedures.Radiology 219:515-520
11. Carlson SK, Felmlee JP, Bender CE, et al (2005) CT fluoroscopy-guided biopsy of the lung or upper abdomen with a breath-hold monitoring and feedback system: a prospective randomized controlled clinical trial. Radiology 237:701-708
12. Sheafor DH, Paulson EK, Kliewer MA, DeLong DM, Nelson RC (2000) Comparison of sonographic and CT guidance techniques. Does CT fluoroscopy decrease procedure time? AJR 174: 939-942
13. Magnusson A, Akerfeldt D (1991) CT-guided core biopsies using a new guidance device. Acta Radiol 32:83-85
14. Palestrant AM (1990) Comprehensive approach to CT-guided procedures with a hand-held guidance device. Radiology 174:270-272
15. Ozdoba C, Voigt K, Nusslin F (1991) New device for CT-targeted percutaneous punctures. Radiology 180:576-578
16. Jacobi V, Thalhammer A, Kirchner J (1999) Value of a laser guidance system for CT interventions; a phantom study. Eur Radiol 9:137-140

17. Wood BJ, Banovac F, Friedman M, et al (2003) CT-integrated programmable robot for image-guided procedures: comparison of free-hand and robot-assisted techniques. J Vasc Interv Radiol 2003;14:S62
18. Besl PJ, McKay ND (1992) A method for registration of 3-D shapes, IEEE Trans Pattern Anal Machine Intelligence 4:239-256
19. van den Elsen PA, Pol EJD, Viergever MA (1993) Medical image matching a review with classification, IEEE Eng Med Biol 2:26-39
20. Sonka M, Fitzpatrick JM (2000) Handbook of Medical Imaging Medical Image Processing and Analysis, SPIE, Bellingham
21. Giraud P, Reboul F, Clippe S, et al (2003) Respiration-gated radiotherapy: current techniques and potential benefits. Cancer Radiother 7:S15–S25
22. Goerres GW, Burger C, Schwitter MR, Heidelberg TN, Seifert B, von Schulthess GK (2003) PET/CT of the abdomen: optimizing the patient breathing pattern. Eur Radiol 13:734–739

LUNG RADIOFREQUENCY ABLATION: IN-VIVO EXPERIMENTAL STUDY WITH PERFUSED MULTINED ELECTRODES

ABSTRACT

Purpose: To investigate feasibility and safety of lung radiofrequency (RF) ablation by using perfused expandable multi-tined electrodes in an in-vivo animal model

Materials and Methods: Ten New Zealand White rabbits underwent RF ablation by using perfused expandable multi-tined electrodes (Starburst Talon, RITA Medical Systems, Mountain View, CA) and 200-W RF generator. The electrode was positioned under fluoroscopy guidance and a single percutaneous RF ablation was performed. Saline perfusate was doped with nonionic iodinated contrast agent to render it visible on computed tomography (CT). An immediate posttreatment CT scanning documented the distribution of the doped saline and the presence of immediate complications. The animals were monitored for delayed complications and sacrificed within 72 hours (n=4), two weeks (n=3), or four weeks (n=3). Assessment of ablation zone and adjacent structures was done at autopsy.

Results: Major complications consisted of pneumothorax requiring drainage (n=2) and skin burn (n=1). Immediately after the procedure the area of ablation was depicted at CT as a round, well-demarcated area, homogenously opacified by iodinated contrast media. The presence of a sharply demarcated area of coagulation necrosis without severe damage to adjacent structures was confirmed at autopsy. In one case, in whom pneumothorax and pleural effusion were depicted, pleural fibrinous adhesions were demonstrated at autopsy.

Conclusion: Lung RF ablation performed in an in-vivo animal model by using perfused expandable multi-tined electrodes is feasible and safe. No severe damage to adjacent structures was demonstrated.

INTRODUCTION

Interventional Oncology is gaining increasing acceptance as a viable alternate or complementary treatment for a variety of cancers. Advances in material science, and methods for delivery of ablating agents combined with improved localization now make possible to be much more aggressive and effective in attempting to achieve local ablation of malignant tumors. Previous studies of saline-enhanced radiofrequency (RF) ablation of the liver have shown that the use of saline allows thermal energy to spread further and faster in tissue, and increases tissue ionicity, thereby permitting greater current flow [1, 2]. The potential benefits of using saline-enhanced RF ablation could be even more important in lung ablation, because of the tissue characteristics of the lung. In fact, air containing lung tissues has a naturally high tissue impedance, and this makes difficult to create a safety margin around the treated lesion [3-6].

On the other hand, direct and uncontrollable thermal damage to adjacent and remote structures was observed more frequently using saline-enhanced RF ablation than with conventional RF in the liver. Saline injected during radiofrequency ablation can extravasate beyond the tumor, and this could result in an undesiderable extension of the ablation zone and complication [7].

The purpose of this investigation is to assess the technical feasibility and safety of percutaneous RF ablation in rabbit lung using a multitined perfused needle.

MATERIALS AND METHODS

STUDY DESIGN

The study was designed as an experimental in-vivo study in rabbit lung. The research protocol was approved by the Animal Research Committee of the

University before initiation of the study. All policies on humane care and use of laboratory animals were followed.

Ten New Zealand White rabbits weighing about 3 Kg each were subjected to RF ablation. After the procedure the animals were carefully monitored for delayed complications and an intramuscolar injection of 100 mg of ampicillin (Amplisol®, Intervet Production, Milan, Italy) was administered from day 1 to day 5 after the procedure. Animals' sacrifices were scheduled at 72 hours (n=4), 2 weeks (n=3) and 4 weeks (n=3) after the procedure.

Following euthanasia, the lungs were harvested in toto, and gross pathology of the ablation zones and adjacent structures were performed.

ABLATION DEVICES

Experiments were performed by using a 200-W generator (model 1500; RITA Medical Systems, Mountain View, CA) and a 15 G RF multitined perfused electrode needle with a central active trocar and 4 side-deploying lateral tines (StarBurst Talon, RITA Medical Systems, Mountain View, CA) connected with a pump (IntelliFlow pump, RITA Medical Systems, Mountain View, CA) to deliver precise amount of saline to the ablation zone (Fig. 1). To perfuse the electrode we used a solution of 200cc of 0.9% NaCl saline doped 12:1 with nonionic iodinated contrast agent (Visipaque®, concentration, 320 mg/ml). The contrast agent, making the solution visible on CT, allowed us to evaluate the saline diffusion in tissues at the CT scan performed after the procedure.

Before inserting the electrode the tines were perfused with the saline doped with the contrast agent at a high flow (0.7 ml/min) by selecting the "Purge mode" on the RF generator. As soon as the saline flowed out of all four tines the purge mode was stopped and the hooks retracted. The generator was put in the "Talon mode " and the pump infused the saline doped with contrast agent into the lateral tines at a rate of 0.1ml/min. The planned ablation was of 3 minutes with the hooks deployed to 2 cm at a target temperature of 105 °C .

ABLATION PROCEDURES

All rabbits were anesthetized by intravenous injection of Zoletil® (tiletamine hypochloride+zolazepam hypochloride, 7 mg/kg) prior to procedures. Booster injections of up to one-half of the initial dose were administrated as needed. The rabbits were able to breath spontaneously during the procedures. The right thoracic wall of each animal were shaved and sterilized, and each animal was placed on left side. A grounding pad was placed in contact with a shaved area on the right haunch.

A marker was placed on the animal's skin at the level of the anticipated needle entry and the correct placement was checked by means of fluoroscopy. After cleansing the needle entry site with povidine-iodine solution a small stab incision was made with a scalpel to facilitate needle entry through the skin. The electrode was inserted directly into the lateral side of the right lower lobe. We chose this approach to reduce the chance of traversing interlobar fissures. After controlling under fluoroscopy the position of the needle in the lung, we deployed hooks up to 2 cm, and we started the ablation (Fig.2). A dedicated software (RITA Base Software, RITA Medical Systems, Mountain View, CA) installed on a portable computer provided graph showing real-time curves of probe-tips temperatures, power output, and tissue impedance throughout the procedures (Fig.3). During the procedure, rabbits were carefully monitored for signs of respiratory distress or discomfort. Following ablation, the probe was removed slowly with a rotatory motion to minimize the potential for tissue disruption.

POST-PROCEDURAL ASSESSMENT

Immediate post-procedural CT scanning was obtained to document the distribution of the doped saline around the ablation zone and check for immediate complications. Axial scans (ST: 3 mm, SP: 1 mm, 120 kVp, 100 mA) of both the lung and upper abdomen, including the kidneys, were obtained. Intravenous

contrast material was not administered. Images were analyzed by using lung windows (level, -500 HU; width, 2000 HU) and soft-tissue windows (level, 50 HU; width, 350 HU).

Imaging Analysis

Ablated lesions was evaluated in terms of location, size and shape, with particular attention to the contrast medium distribution around the ablation area. We evaluate also the presence of effusion in the pleural cavity or air in the pleural cavity or in soft tissues. The diameters of the ablated lesions were measured on PACS, on lung window images, by one radiologist using an electric caliper. To ensure that the changes noted were not present before RF ablation, the post- and preprocedural CT findings were compared.

Histopathologic Examination

After euthanasia the rabbits' lungs and heart were harvested. The lung gross specimens obtained were dissected in planes similar to those of the CT scans, and were examined measuring the central discolored region of coagulation necrosis in each pathologic specimen.

RESULTS

All procedures were technically successful (10/10 animals, 100%) and completed according to protocol. Rabbits tolerated the procedure well. All rabbits awoke quickly from anesthesia, and normal activity and weight gain were observed during daily monitoring.

Major complications occurring were pneumothorax requiring drainage (n=2) and skin burn (n=1) (Fig.4). The pneumothoraces occurred acutely and were observed after needle insertion, before starting the ablations. A skin burn was observed in the right haunch of one rabbit when the grounding pad was removed.

Minor complications included mild pneumothorax (n=1) and pleural effusion (n=1) not requiring drainage, and pneumothorax with pleural effusion in the same animal (n=1) not requiring treatment. No delayed complications were observed.

At the immediate postprocedural CT, a round well demarcated ablation zone (mean size 2.3 cm ± 0.8) is evident, with internal homogeneous distribution of iodinated contrast media in 10/10 cases (Fig.5). Iodinated contrast agent was not depicted at post-procedural CT in adjacent lung parenchima, in bronchi, mediastinum, pleural or abdominal cavity (Fig.6).

At gross pathology a clear-cut, sharply demarcated coagulation necrosis area (mean size, 2.1 cm ± 0.4) was evident (Fig.7). Clear-cut, sharply demarcated coagulation necrosis was observed in the animals sacrificed 72 hours or more after the procedure. Coagulation necrosis was initially surrounded by a reddish hyperemic rim. After 15 days, the hyperemic halo was no longer seen, and the lesion was surrounded by a firm, fibrotic, white peripheral rim. No significant differences at histopathology were demonstrated in ablation zone organization between specimen collected 2 and 4 weeks after the procedures. In all cases, lung parenchyma adjacent and far from the thermal lesion did not present any grossly apparent abnormality. In one case, in whom pneumothorax and pleural effusion were depicted, pleural fibrinous adhesions were demonstrated at autopsy (Fig.8). No severe damage of organs adjacent to the lungs was observed. In particular heart, pericardium and diaphragm were non injured (Fig.8). Major arterial and venous pulmonary vessels were preserved, in the absence of sign of thrombosis or parietal damage.

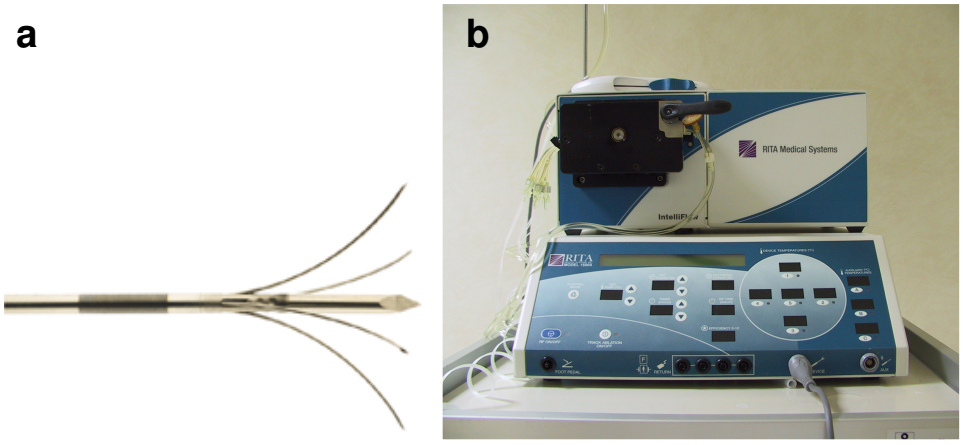

Fig. 1(a,b). 15 G RF multitined perfused electrode needle with a central active trocar and 4 side-deploying lateral tines (a) was connected with a 200-W generator and a with a pump (b)

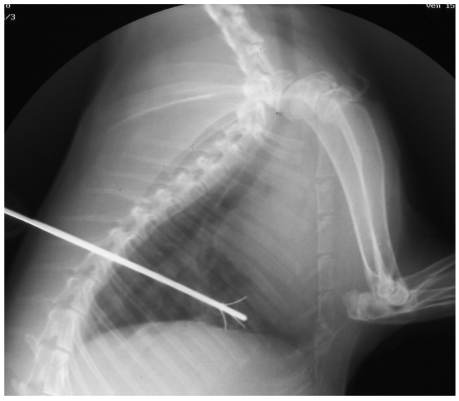

Fig. 2. The electrode was placed under fluoroscopy guidance and the times were deployed to 2 cm

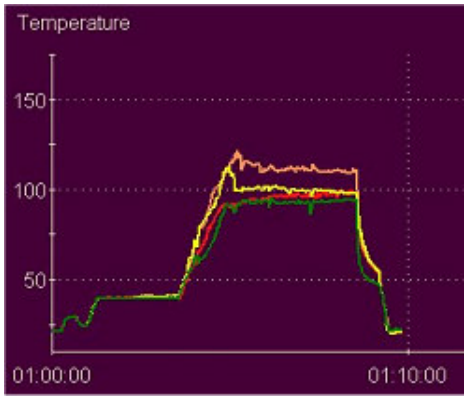

Fig. 3. A dedicated software i provided graph showing real-time curves of probe-tips temperatures

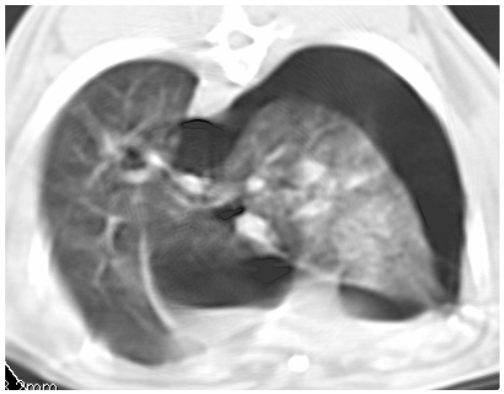

Fig. 4. Severe pneumothorax that occurred immediately after needle insertion, before starting ablation

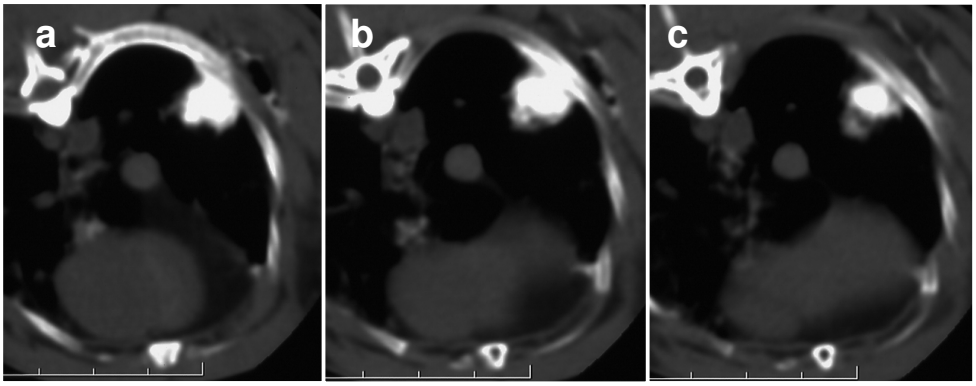

Fig. 5 (a-c). At the immediate postprocedural CT, a round well demarcated ablation zone is evident, with internal homogeneous distribution of iodinated contrast media

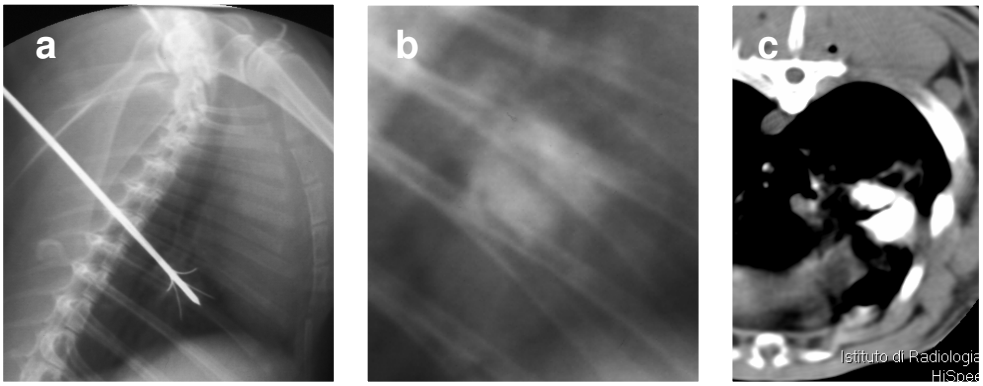

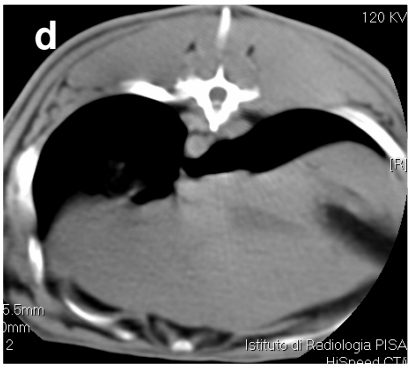

Fig. 6 (a-d). After electrode placement in the right lower lobe and the deployment of the hooks under fluoroscopy guidance (a) the ablation is started. At the end of the ablation an opacified area was depicted ar fluoroscopy (b). At the immediate postprocedural CT, a round well demarcated ablation zone is evident,opacified by the iodinated contrast media (c). Contrast media was not depicted in pleural cavity .

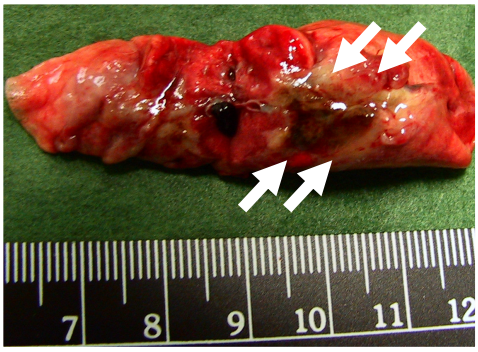

Fig. 7. At gross pathology a clear-cut, sharply demarcated coagulation necrosis area was evident

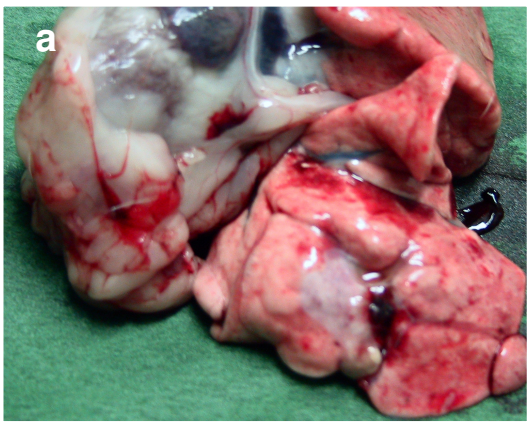

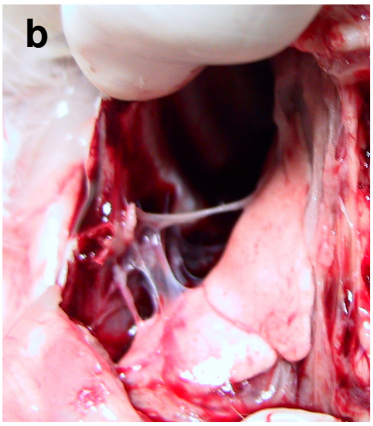

Fig. 8 (a,b). Lung parenchyma adjacent and far from the thermal lesion did not present any grossly apparent abnormality (a). In one case, in whom pneumothorax and pleural effusion were depicted, pleural fibrinous adhesions were demonstrated at autopsy (b).

DISCUSSION

Lung cancer is among the most common malignancies in the world and is the leading cause of cancer death [8, 9]. For patients with stage I and II non-small cell lung cancer (NSCLC), surgical resection is usually regarded as the treatment of choice. The most frequent reasons for denying surgery in these patients are associated comorbidity, patient refusal to undergo surgery, or advanced age. The presence of severe comorbidity in NSCLC patients is increasing owing to the increase of lung cancer incidence among the elderly as a consequence of increased life expectancy [10-12]. In addition, NSCLC tends to recur even after successful resection [13]. Chemotherapy and radiation therapy protocols are used to treat patients with non-operable or unresectable tumors, but have not been entirely satisfactory in terms of long-term survival outcomes [12, 14].

Lungs are also the second most frequent site of metastatic disease. There have been multiple series documenting survival benefits in patients with pulmonary metastases of favourable histology who were completely resected as compared to unresectable individuals [15,16]. However, surgery is frequently precluded by the number and location of metastatic nodules. Moreover, the high risk of recurrence in patients with metastatic disease and the need to remove functioning lung tissue along with the lesions limit the indications for surgery [17]. In these cases, radiation therapy and palliative chemotherapy are offered. Yet, both of these treatment options can further damage the pulmonary parenchyma and offer little hope for a cure [18]**.** Therefore, new modalities for local treatment that effectively destroy tumor but are less invasive and less damaging to normal lung tissue are required.

Percutaneous RF ablation is presently the most frequently used technique to treat solid tumors, thanks to its effectiveness, safety and relative ease of use. Because of its ability to produce large volumes of coagulation necrosis in a controlled fashion, this technique has gained acceptance as viable therapeutic option for unresectable liver malignancies [19,20]. Recently, investigation has

been focused on the clinical application of RF ablation in the treatment of lung malignancies [21-23]. Lencioni et al. [24] reported the results of a multicenter trial in which 106 patients with 186 malignant lung tumors 3.5 cm in diameter or smaller were treated. Diagnoses included NSCLC in 33 patients, metastasis from colorectal cancer in 53, and metastasis from other primary malignancy in 20. Complete ablation of macroscopic tumor as shown by 3-month CT was achieved in 173 of 186 tumors (primary effectiveness rate, 93%), with an overall survival was 69% and 49% at 1 and 2 years respectively in patients with NSCLC; 86% and 62% at 1 and 2 years in patients with colorectal cancer metastases. Cancer-specific survival was 91% and 91% at 1 and 2 years in patients with NSCLC; 88% and 72% at 1 and 2 years in patients with colorectal metastases.

A limitation of RF ablation is that, as temperatures reach 100° C and boiling occurs, increased impedance limits further deposition of electricity into tissue [25]. This becomes even more pronounced if charring occurs; the resultant eschar forms a highly effective insulator around the electrode. In addition air containing lung tissue has a naturally high impedance. Several different types of electrodes have been developed to avoid this effect and increase tissue heating and coagulation during RF ablation. These include internal water-cooling, and multi-tined electrode designs [26-27]. Saline injected either before or during RF ablation has also been used to increase the size of the ablation zone [28]. Saline acts as a wet electrode increasing the total effective electrode size, reduces tissue dehydration and charring, and hence produces a larger ablation zone [29,30]. It was however noted that adjunctive saline resulted in a more irregular ablation zone and that saline can extravasate beyond the tumor. With the high-perfusion-rate system this could result in an undesirable extension of the ablation zone and a complication [7, 31, 32].

Our concern was that saline infused during RF ablation of lung tumors may not always be confined to the tumor. Our aim was to demonstrate the distribution of saline after ablation with perfused electrodes in an experimental animal model.

In our study all procedures were technically successful and the animals well tolerated the procedures. Severe and mild pneumothoraces, the most frequent complication, were puncture-related and occurred before starting the ablation. Therefore they were not related to the infusion of saline during RF ablation. No delayed complications were observed. At the immediate postprocedural CT, a round well demarcated ablation zone was evident, with internal homogeneous distribution of iodinated contrast media in all cases. Iodinated contrast agent was not depicted at post-procedural CT in adjacent lung parenchima, in bronchi, mediastinum, pleural or abdominal cavity. These findings were confirmed at autopsy where lung parenchyma adjacent and far from the thermal lesion did not present any grossly apparent abnormality and no severe damage of organs adjacent to the lungs was observed. In particular heart, pericardium and diaphragm were non injured. Major arterial and venous pulmonary vessels were preserved, in the absence of sign of thrombosis or parietal damage. The safety of the procedure could be related to the controlled, slow infusion of saline during ablation. The dedicated infusion pump allows the lateral tines to be perfused by saline with a slow, constant flow of 0,1 ml/min. To our knowledge this is the first report concerning the use of Talon electrode combined with Intellyflow pump in lung tissue. The micro-perfusion could represent the most important factor to guarantee the safety of the procedure.

A study performed in rabbit lung showed that saline infusion during lung RF ablation was associated with lower impedance, higher power delivery and larger lesion size [6]. In this study the incidence of complications, and in particular of pneumothoraces, tended to be higher in the group of animals submitted to RF and saline instillation, even if the difference was not statistically significant. The reason was probably in the fact that the Author used a Chiba needle to infuse the saline and thus they punctured at least twice the pleura. However the shape of the ablation zone was spherical using small amounts of saline, and this was probably due, as in our study, to the slow flow of saline infusion that was approximately of 0.05 ml/min. When RF ablation was performed in the porcine lung using a

perfusion electrode with a relatively high flow of saline (1.5 ml/min) it was in fact demonstrated that the coagulation volume was larger that that obtained with internally cooled or multitined expandable electrodes, but that the ablation zone had irregular margins [33].

Our study has however some limitations. First, the results obtained in healthy rabbit lung may differ from those obtained with non-small-cell lung carcinoma or lung metastses in humans. Second, the safety of the procedure was evaluated clinically and on the basis of post procedural CT and gross pathology examination, without performing histological examination. We were however not assessing the ability of the device to produce ablation in lung tissue: In view of the small size of rabbit lungs Talon electrode was deployed to 2 cm, actually half its maximum deplyment. Third, since the 15G electrode used in this study is large for rabbits, with their relatively smaller lungs, the complication rates of RFA might be overestimated.

In conclusion, CT-guided percutaneous RF ablation performed with perfused multitined electrodes is feasible and safe. Saline-enhanced RF ablation might be a promising technique for the management of inoperable lung malignancies and has the potential for use as a minimally invasive approach. To determine whether the technique can be feasibly and safely used to produce a sufficiently large volume of necrosis to be of value in the treatment of small peripheral lung tumors in patients for whom surgery or palliative radiotherapy is unsuitable, further study using a larger animal model is warranted.

REFERENCES

1. Miao Y, Ni Y, Mulier S, et al (1997) Ex-vivo experiment on radiofrequency liver ablation with saline infusion through a screw-tip cannulated electrode. J Surg Res 71:19-24
2. Livraghi T, Goldberg SN, Monti F, et al (1997) Saline-enhanced radiofrequency tissue ablation in the treatment of liver metastases. Radiology 202:205–210
3. Goldberg SN, Gazelle GS, Compton CC, el al (1995) Radiofrequency tissue ablation in the rabbit lung: efficacy and complications. Acad Radiol 2:776-784
4. Goldberg SN, Gazelle GS, Compton CC, el al (1996) Radiofrequency tissue ablation of VX2 tumor nodules in the rabbit lung. Acad Radiol 3:929-935
5. Miao Y, Ni Y, Bosmans H, et al (2001) Radiofrequency ablation for eradication of pulmonary tumor in rabbits. J Surg Res 99:265-271
6. Lee JM, Kim SW, Li CA, et al (2002) Saline-enhanced radiofrequency thermal ablation of the lung: a feasibility study in rabbits. Korean J Radiol 3:245-253
7. Gillams AR, Lees WR (2005) CT mapping of the distribution of saline during radiofrequency ablation with perfusion electrodes. Cardiovasc Intervent Radiol 28:476–480
8. Ginsberg RJ, Vokes EE, Raben A (1997) Cancer of the lung: Non-small cell lung cancer. In: Cancer: Principles and Practice of Oncology, 5th ed. Philadelphia, PA: Lippincott-Raven Publishers; pp 849-857
9. Fry WA, Phillips JL, Menck HR (1999) Ten-year survey of lung cancer treatment and survival in hospitals in the United States: a national cancer data base report. Cancer 86: 1867-1876
10. Birim O, Kappetein AP, Goorden T, van Klaveren RJ, Bogers AJ (2005) Proper treatment selection may improve survival in patients with clinical early-stage nonsmall cell lung cancer. Ann Thorac Surg 80:1021-1026
11. Iwasaki A, Shirakusa T, Enatsu S, Maekawa S, Yoshida Y, Yoshinaga Y (2005) Surgical treatment for lung cancer with COPD based on the Global Initiative for Chronic Obstructive Lung Disease (GOLD). Thorac Cardiovasc Surg 53:162-167
12. Rowell NP, Williams CJ (2001) Radical radiotherapy for stage I/II non-small cell lung cancer in patients not sufficiently fit for or declining surgery (medically inoperable): a systematic review. Thorax 56:628-638
13. Rice D, Kim HW, Sabichi A, et al (2003) The risk of second primary tumors after resection of stage I non-small-cell lung cancer Ann Thor Surg 76: 1001-1008
14. Clegg A, Scott DA, Sidhu M, Hewitson P, Waugh N (2001) A rapid and systematic review of the clinical effectiveness and cost-effectiveness of

paclitaxel, docetaxel, gemcitabine and vinorelbine in non-small-cell lung cancer. Health Technol Assess 5:1-195
15. Inoue M, Kotake Y, Nakagawa K, et al (2000) Surgery for pulmonary metastases from colorectal carcinoma. Ann Thorac Surg 70: 380-383
16. Pastorino U, Buyse M, Godehard F, et al. for the International Registry of Lung Metastases (1997) Long-term results of lung metastasectomy: prognostic analysis based on 5206 cases. J Thorac Cardiovasc Surg 113: 37-49
17. Kandolier D, Kromer E, Tuchler H, et al (1998) Long-term results after repeated surgical removal of pulmonary metastases. Ann Thorac Surg 65: 909-912
18. Elias A (1993) Chemotherapy and radiotherapy for regionally advanced non-small-cell lung cancer. Chest 103(Suppl 4): 362-366
19. Dodd GD III, Soulen MC, Kane RA, et al (2000) Minimally invasive treatment of malignant hepatic tumors: at the threshold of a major breakthrough. RadioGraphics 20: 9-27
20. Lencioni R, Cioni D, Bartolozzi C (2001) Percutaneous radiofrequency thermal ablation of liver malignancies: technique, indications, imaging findings and clinical results. Abdom Imaging 26: 345-360
21. Dupuy DE, Mayo-Smith WW, Di Petrillo T, et al (2001) Clinical experience of pulmonary radiofrequency ablation in 27 patients. Radiology 221(P): 389
22. Kang S, Lao R, Liao W, et al (2001) Effect of radiofrequency ablation on lung cancer. ASCO Program/Proceedings 20: 1342
23. de Baere T, Palussiere J, Auperin A, et al (2006) Midterm local efficacy and survival after radiofrequency ablation of lung tumors with minimum follow-up of 1 year: prospective evaluation. Radiology 240: 587-596
24. Lencioni R, Crocetti L, Cioni R, et al (2006) Radiofrequency ablation of pulmonary tumors response evaluation (RAPTURE) trial: final report. European Congress of Radiology (ECR) Annual Meeting 2006
25. Goldberg SN, Gazelle GS, Solbiati L, et al (1996) Radiofrequency tissue ablation: increased lesion diameter with a perfusion electrode. Acad Radiol 3: 636-644
26. Rossi S, Buscarini E, Garbagnati F, et al (1998) Percutaneous treatment of small hepatic tumors by an expandable RF needle electrode. AJR Am J Roentgenol 170: 1015-1022
27. Goldberg SN, Solbiati L, Hahn PF, et al (1998) Large-volume tissue ablation with radiofrequency by using a clustered, internally cooled electrode technique: laboratory and clinical experience in liver metastases. Radiology 209: 371-379
28. Livraghi, T, Goldberg, SN, Monti, F, Bizzini, A, Lazzaroni, S, Meloni, F, Pellicano, S, Solbiati, L, Gazelle, GS (1997) "Saline-enhanced radio-frequency tissue ablation in the treatment of liver metastases" Radiology 202: 205-210

29. Gananadha, S, Morris, DL (2004) "Saline infusion markedly reduces impedance and improves efficacy of pulmonary radiofrequency ablation" Cardiovasc Intervent Radiol 27: 361-365
30. Goldberg SN, Ahmed M, Gazelle GS, et al (2001) Radiofrequency thermal ablation with NaCl solution injection: effect of electrical conductivity on tissue heating and coagulation—phantom and porcine liver study. Radiology 219:157-165
31. de Baere, T, Dromain, C, Kuoch, V, Elias, D, Kardache, M, Roche, A (2001) "Radiofrequency ablation of liver tumours: Four years of single-centre experimental work and clinical practice" Radiology 221: 653
32. Kim TS, Lim HK, Kim H (2006) Excessive hyperthermic necrosis of a pulmonary lobe after hypertonic saline-enhanced monopolar radiofrequency ablation. Cardiovasc Intervent Radiol. 29:160-163
33. Lee JM, Han JK, Chang JM, et al (2006) Radiofrequency ablation in pig lungs: in vivo comparison of internally cooled, perfusion and multitined expandable electrodes. Br J Radiol 79: 562-572

THERMAL ABLATION OF THE LUNG: IN VIVO EXPERIMENTAL COMPARISON OF MICROWAVE AND RADIOFREQUENCY

ABSTRACT

Purpose: To compare feasibility, safety and effectiveness of microwave (MW) ablation versus radiofrequency (RF) ablation in a lung rabbit model.

Methods and Materials: Twenty New Zealand White rabbits were submitted to either MW ablation (n=10, group A) or RF ablation (n=10, group B). A single percutaneous ablation of lung tissue was performed in each animal under computed tomography (CT) guidance. The procedures were carried out with a prototype MW ablation device (Vivawave; Tyco Healthcare) and a commercially available RF ablation system (Cool-tip; Tyco Healthcare). Animals' sacrifices were scheduled at 3 days (group A, n=5; group B, n=5) and 7 days (group A, n=5; group B, n=5) after the procedure. Gross pathology and microscopic assessment of the ablation zones and adjacent structures were performed.

Results: Technical success was achieved in 9/10 rabbits in group A and 9/10 rabbits in group B. Technical failures were related to intra-procedural animal death due to anaesthesiology stress (n=1, group A) and severe pneumothorax (n=1, group B). One rabbit of group B died 24 hours after the procedure because of massive hemothorax. Complications included pneumothorax (group A, n=4; group B, n=4), abscess (group A, n=1; group B, n=1), and thoracic wall burn (group A, n=4). The mean diameter of the ablation zone on gross examination were 12.1mm ± 3.2 in group A and 14.8 mm ± 4.9 in group B (p=0.2). At histopathology, zones of thermal injuries in group A and B were similar, with septal necrosis, edema, hemorrhage and peripheral lymphocytic infiltrate. Thrombosis of small vessels surrounding the ablation zone was extensively depicted in group A specimens and focally present in group B specimens. No severe damage of adjacent organs was observed.

Conclusion: Feasibility and safety of MW ablation are similar to those of RF ablation in a lung rabbit model. MW and RF ablated zones are similar in pathologic appearance. MW ablation produces a greater damage to peripheral small vessels inducing thrombosis.

INTRODUCTION

Radiofrequency (RF) ablation is a relatively new minimally invasive technique used to treat solid tumors. It has become a desired image-guided ablative method because of its ability to produce large regions of coagulative necrosis in a controlled fashion. Following recent advances in the RF technology, RF ablation has gained an increasingly important role in the treatment of unresectable hepatic malignancies, and is challenging partial hepatectomy as the treatment of choice for patients with limited hepatic tumor [1-3]. Despite the experience with RF ablation of malignant tumors outside the liver being at an early stage of clinical application, recent studies have shown that this technique could offer a valuable treatment option for unresectable lung malignancies [4-10].

However, RF ablation is fundamentally restricted by the need to conduct electric energy into the body. As temperatures reach 100°C and boiling occurs, increased impedance limits further deposition of electricity into tissue [11]. This becomes even more pronounced if charring occurs. A further limitation of RF ablation is the relatively small zone of active heating created by ionic agitation [12]. The majority of tissue heating is thus due to thermal conduction, which decreases exponentially away from the source. The high rate of local recurrence seen in some clinical series of RF ablation is almost certainly caused in part by the protective effect of blood flow in the liver, termed the "heat-sink effect" [13].

With several theoretic and practical advantages, microwave (MW) ablation is a promising new option in the treatment of surgically unresectable tumors. The potential benefits of MW technology include consistently higher intratumoral

temperatures, larger tumor ablation volumes, faster ablation times, improved convection profile and less procedural pain [14-17]. Because the cooling effect of blood flow is most pronounced within the zone of conductive rather than active heating, a larger power field may also enhance treatment of perivascular tissue [16,17]. Recent advances in MW engineering have allowed the design of new MW systems with the potential for larger, more controlled ablation zones. We considered it essential to know how MW ablation affects normal lung tissue before performing clinically for peripheral lung malignancies. An experimental study was deemed necessary to evaluate the thermal response, coagulation extent, and histological changes in the air-filled normal lung. Demonstration of the ability of MW ablation to destroy normal lung tissue is clinically relevant, as it would enable creation of a safety margin of ablation of pulmonary parenchyma around lung tumors, which is expected to result in higher rates of complete tumor eradication and lower rates of local recurrence. Thus, the purpose of our study was to compare a prototype MW ablation system with a commercially available RF device in an in-vivo lung rabbit model.

METHODS AND MATERIALS

STUDY DESIGN

Our institutional Animal Research Committee gave protocol approval for this study. All policies on humane care and use of laboratory animals were followed. Twenty New Zealand White rabbits were divided into two groups. Group A (n=10) was submitted to single percutaneous MW ablation. Group B (n=10) received single percutaneous RF ablation.

After the procedure the animals were carefully monitored for delayed complications and an intramuscolar injection of 100 mg of ampicillin (Amplisol®, Intervet Production, Milan, Italy) was administered from day 1 to day 5 after the

procedure. Animals' sacrifices were scheduled at 3 days (group A, n=5; group B, n=5) and 7 days (group A, n=5; group B, n=5) after the procedure.

Following euthanasia, the lungs were harvested in toto, and gross pathology and microscopic assessment of the ablation zones and adjacent structures were performed.

ABLATION DEVICES

The MW ablation device used in this study is a prototype developed by Tyco Healthcare. The antenna is a 15-gauge coaxial dipole design with a 1.6-cm exposed tip (Vivawave, Tyco Healthcare). A MW generator is used to drive the system at 915 MHz, with power output controlled by means of a laptop computer with custom software. MW ablation was planned to be performed at a power of 45 W for a duration of 10 minutes.

RF ablation was performed with a 17-gauge, 2-cm exposed-tip RF electrode (Cool-tip, Tyco Healthcare). Ablation area was created using a RF generator capable of producing 200 W power. Tissue impedance was monitored by circuitry incorporated within the generator. A peristaltic pump was used to infuse normal saline solution at 0° C into the lumen of the electrode at a rate of 10-25 ml/min. RF ablation was planned to be performed for a duration of 12 minutes.

ABLATION PROCEDURES

All rabbits were anesthetized by intravenous injection of 7 mg/kg of tiletamine hypochloride+zolazepam hypochloride (Zoletil®) prior to procedures. Booster injections of up to one-half of the initial dose were administrated as needed. The rabbits were able to breath spontaneously during the procedures.

The right thoracic wall of each animal were shaved and sterilized, and each animal was placed on left side. In group B rabbits a pediatric grounding pad was placed in contact with a shaved area on the right haunch. Positioning of the

grounding pad was adjusted to minimize initial circuit impedance. In group A animals, who underwent MW ablation, positioning of grounding pad is not necessary because of the inherent properties of the electromagnetic wave.

Both MW and RF procedures were performed following standard rules for computed tomography (CT)-guided lung biopsy. CT scanning was performed with a dedicated machine for experimental studies (CT Sytec 3000, GE Medical System) operating in standard axial mode. Parameters included 5mm section collimation, 120 kVp, 100 mA and a high resolution matrix filter. A marker was placed on the animal's skin avoiding the great dorsal vein, at the level of the anticipated needle entry, and the correct placement was checked by means of CT.

After cleansing the needle entry site with povidine-iodine solution, a small stab incision was made with a scalpel to facilitate needle entry through the skin. The electrode was inserted directly into the lateral side of the right lower lobe. We chose this approach to reduce the chance of traversing interlobar fissures (Fig. 1). During the procedure, rabbits were carefully monitored for signs of respiratory distress or discomfort. Following ablation, the probe was removed slowly with a rotatory motion to minimize the potential for tissue disruption.

POST-PROCEDURAL ASSESSMENT

Using the same scanner, immediate post-procedural CT scanning was obtained to assess the ablation zone and check for immediate complications. Axial scans (5mm section collimation, 120 kVp, 100 mA) of both the lung and upper abdomen, including the kidneys, were obtained. Intravenous contrast material was not administered. Images were analyzed by using lung windows (level, -500 HU; width, 2000 HU) and soft-tissue windows (level, 50 HU; width, 350 HU).

Imaging Analysis

Each MW and RF ablation zones was evaluated in terms of its location, size and shape, attenuation change, and the presence of effusion in the pleural cavity or air

in the pleural cavity or in soft tissues. The diameters of the ablated lesions were measured on lung window images, by one radiologist, using an electronic caliper. To ensure that the noted changes were not present before MW and RF ablation, the pre- and postprocedural and CT findings were compared.

Histopathologic Examination

After euthanasia the rabbits' lungs and heart were harvested en-block. The lung gross specimens obtained were dissected in planes similar to those of the CT scans, and were examined. For macroscopic examination, the pathologist measured the central discolored region of coagulation necrosis in each pathologic specimen. Tissues were then fixed in 10% formalin for routine histological examination, and final processing for light microscopic study involved paraffin sectioning and haematoxylin-eosin (HE) staining. Tissues obtained from all treatment areas were analyzed for non-viability, their histological appearance, and demarcation from surrounding viable tissue.

DATA ANALYSIS

The technical aspects of MW and RF ablation and complications arising after both kind of procedures were compared. The size of the MW and RF ablation zones at immediate CT scan and at pathology were compared using an unpaired Student's t test. For statistical analysis, JMP 5.0.1.2 computer software (SAS Institute Inc, Cary, NC, USA) was used and a p value of less than 0.05 was considered statistically significant.

RESULTS

Technical success was achieved in 9/10 rabbits in group A and 9/10 rabbits in group B. Technical failure in group A was related to intra-procedural animal death

due to anaesthesiology stress. The animal expired at 6 minutes after the start of the procedure and ablation was allowed to complete. Post-procedural CT demonstrated no pneumothorax and the animal was autopsied immediately. After inspection of the thoracic cavity, there appeared to be a normal ablation that did not involve the heart. The section was removed and was analyzed for histology. Technical failure in group B was due to severe pneumothorax, causing electrode misplacement. Percutaneous drainage was performed but the pneumothorax remained severe and the animal died.

One rabbit of group B died 24 hours after the procedure because of massive hemothorax, that was depicted at CT performed immediately after the procedure and confirmed at autopsy (Fig. 2).

Complications included pneumothorax (group A, n=4; group B, n=4), abscess (group A, n=1; group B, n=1), and thoracic wall burn (group A, n=4). All pneumothoraces occurred acutely and were observed after needle insertion, before starting the ablations. Pneumothoraces observed in group A were all of mild entity and did not require any specific treatment. All the procedures were completed in these animals. One out of four pneumothoraces observed in group B animals was severe and needed drainage. The animal was rescheduled for the RF procedure that was successfully performed 2 weeks later. In 3 cases the pneumothoraces were limited and managed conservatively (Fig. 3).

Both the abscesses occurred in the periprocedural period, and were demonstrated at autopsy performed 7 days after the procedure. Purulent material was present in the right emithorax of one rabbit of the group submitted to MW and in one animal submitted to RF (Fig. 4a). The appearance and the entity of the abscesses were similar in the two animals.

Thoracic wall burns were observed in 4 out of 10 animals in group A (Fig. 4b). All of them were in the site of needle entry where, during the procedure, the skin was heated up together with the needle shaft and the cable.

MW and RF ablation zones were indistinguishable at immediate CT. Immediately after MW or RF ablation, a restricted area of central dense opacity

enclosed by an extensive area of ground-glass opacity was noted in the ablated region on CT images (Fig. 5).

The mean longest diameter of the ablated lesions at CT images acquired immediately after the procedure were 18.8 ± 5.4 mm in group A and 20.4 ± 4.0 mm in group B (p=0.3).

At autopsy, no severe damage of organs adjacent to the lungs was observed. In particular heart, pericardium and diaphragm were non injured. Major arterial and venous pulmonary vessels were preserved, in the absence of sign of thrombosis or parietal damage.

The mean longest diameter of the ablation zone on gross examination was 12.1mm ± 3.2 in group A and 14.8 mm ± 4.9 in group B (p=0.2). At histopathology, zones of thermal injuries in group A and B were similar, with septal necrosis, edema, hemorrhage and peripheral lymphocytic infiltrate (Fig. 6). No significant differences at histopathology were demonstrated in ablation zone organization between specimen collected at 3 and 7 days after the procedures. Thrombosis of small vessels surrounding the ablation zone was extensively depicted in group A specimens and focally present in group B specimens (Fig. 7).

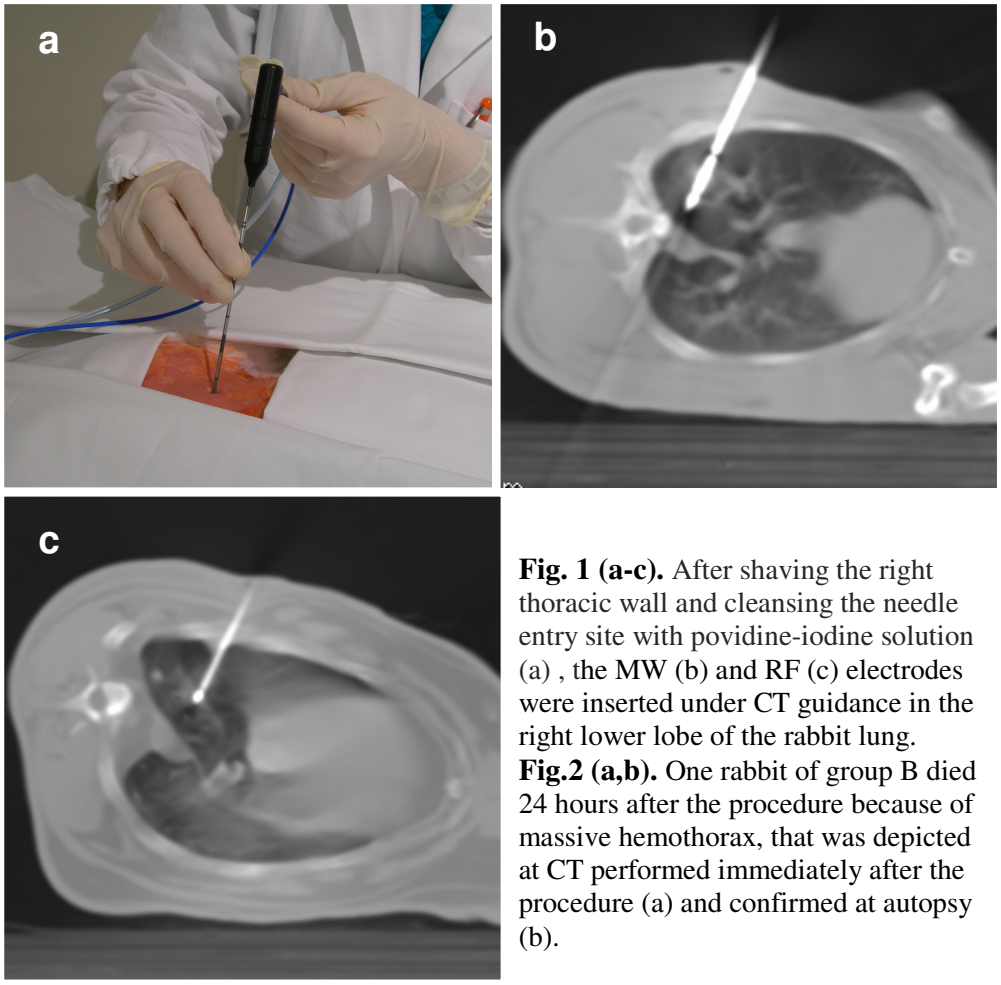

Fig. 1 (a-c). After shaving the right thoracic wall and cleansing the needle entry site with povidine-iodine solution (a) , the MW (b) and RF (c) electrodes were inserted under CT guidance in the right lower lobe of the rabbit lung.
Fig.2 (a,b). One rabbit of group B died 24 hours after the procedure because of massive hemothorax, that was depicted at CT performed immediately after the procedure (a) and confirmed at autopsy (b).

Fig.1

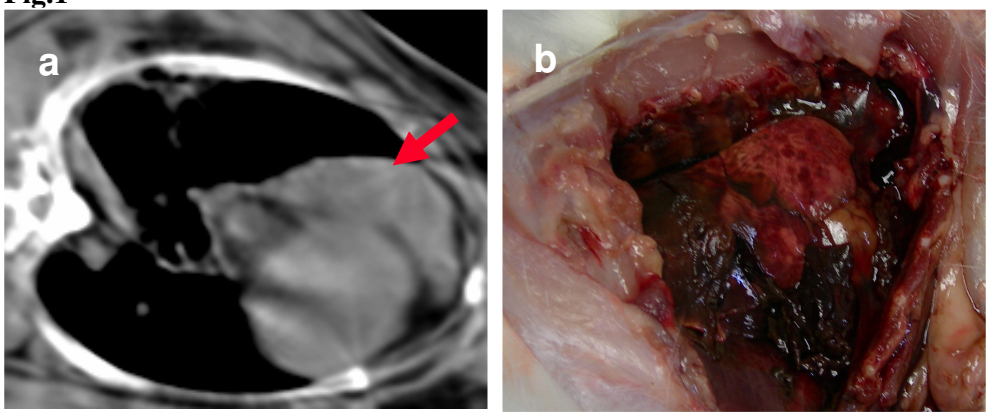

Fig.2

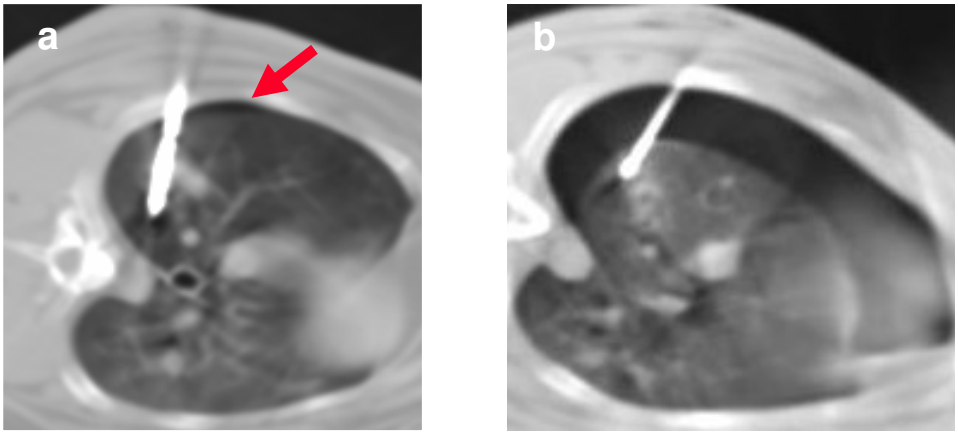

Fig. 3 (a,b). Pneumothorax of mild entity in a rabbit of the group submitted to MW (a). Severe pneumothorax in an animal submitted to RF.

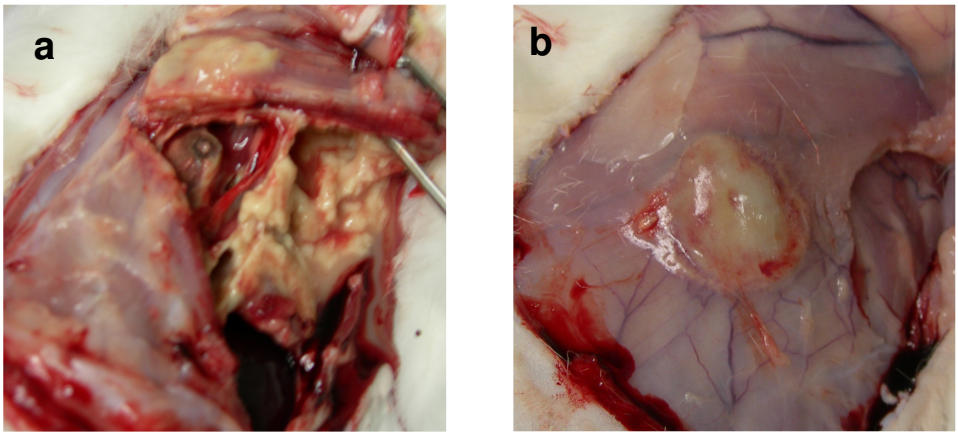

Fig. 4 (a,b). Purulent material in the right emithorax of one rabbit of the group submitted to MW (a); thoracic wall burn (b) in one animal of the MW group

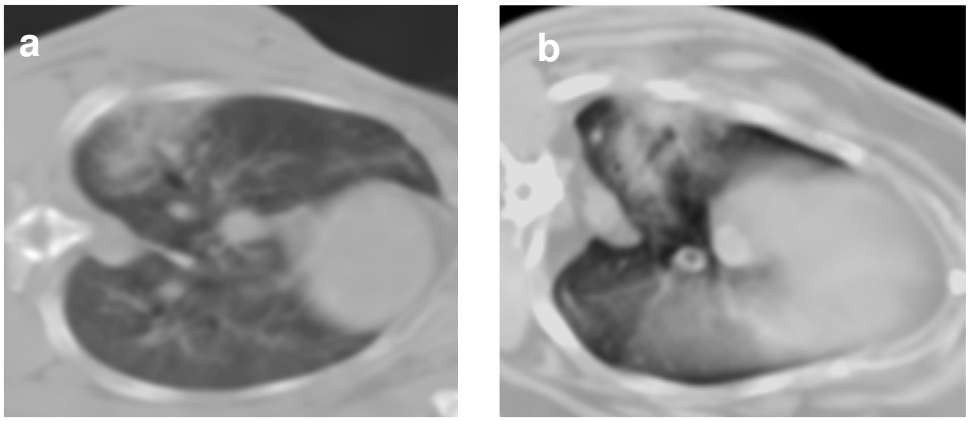

Fig. 5 (a,b). MW (a) and RF (b) ablation zones were indistinguishable at immediate CT

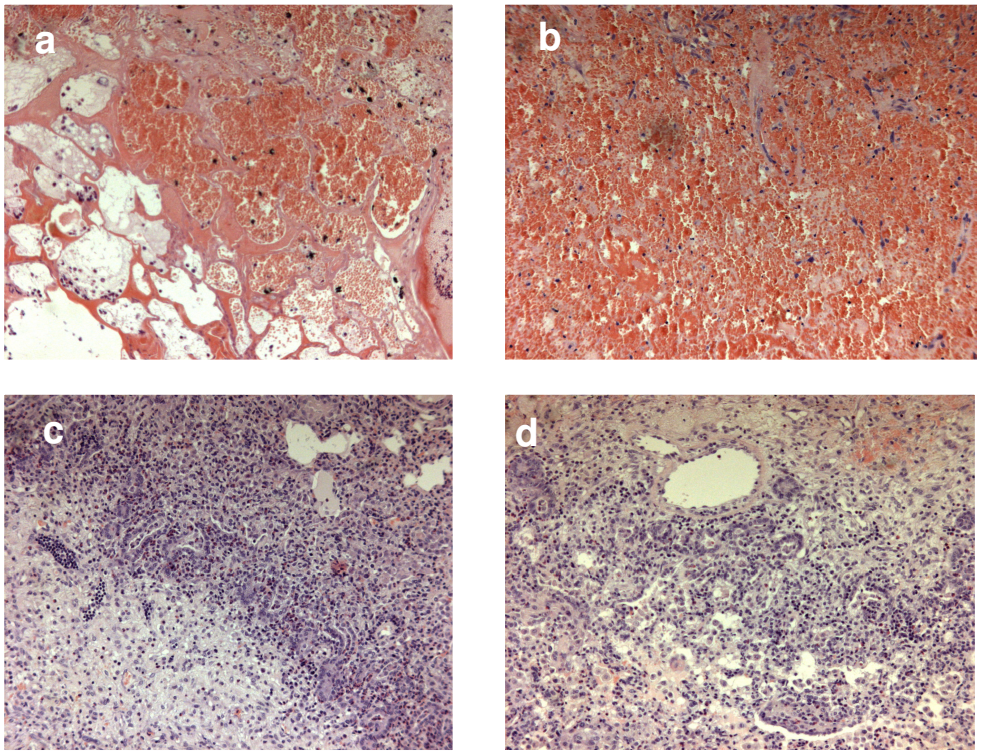

Fig. 6 (a-d). Similar findings of septal necrosis, edema, hemorrhage were depicted at histopathology in specimens collected both 3 and 7 days after MW (a) and RF (b). Lymphocytic infiltrate was present peripherally in specimens of the two groups (c, MW; d, RF)

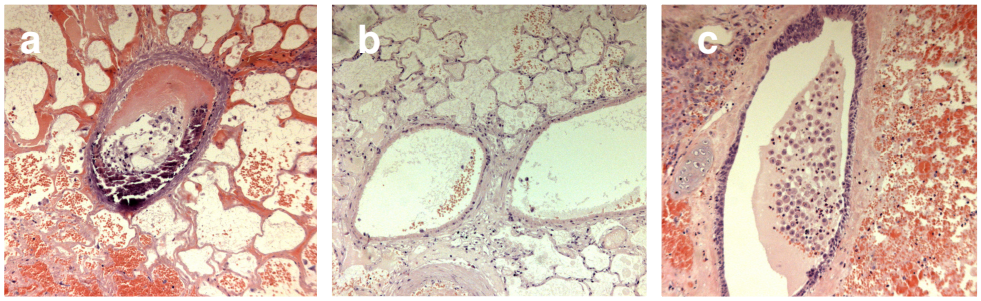

Fig. 7 (a-c). Thrombosis of small vessels surrounding the ablation zone was extensively depicted in specimens of animal submitted to MW (a). In animals submitted to RF vessels without thrombosis (b) together with vessels with partial thrombosis (c) were depicted.

DISCUSSION

Lung cancer is among the most common malignancies in the world and is the leading cause of cancer death [18, 19]. Surgical resection is the treatment of choice for early-stage non-small cell lung cancer (NSCLC). Unfortunately, patients with early-stage NSCLC are sometimes poor surgical candidates, because of co-existent chronic obstructive bronchopneumopathy or other associated diseases [20-22]. In addition, NSCLC tends to recur even after successful resection [23]. Thanks to widespread use of CT small pulmonary nodules (3 cm or less in diameter) are now being diagnosed more frequently [18, 19, 24, 25]. Chemotherapy and radiation therapy protocols are used to treat patients with non-operable or unresectable tumors, but have not been entirely satisfactory in terms of long-term survival outcomes [22,26].

Lungs are also the second most frequent site of metastatic disease. There have been multiple series documenting survival benefits in patients with pulmonary metastases of favourable histology who were completely resected as compared to unresectable individuals [27, 28]. However, surgery is frequently precluded by the number and location of metastatic nodules. Moreover, the high risk of recurrence in patients with metastatic disease and the need to remove functioning lung tissue along with the lesions limit the indications for surgery [29]. In these cases, radiation therapy and palliative chemotherapy are offered. Yet, both of these treatment options can further damage the pulmonary parenchyma and offer little hope for a cure [30]**.** Therefore, new modalities for local treatment that effectively destroy tumor but are less invasive and less damaging to normal lung tissue are required.

Percutaneous RF ablation is presently the most frequently used technique to treat solid tumors, thanks to its effectiveness, safety and relative ease of use. Because of its ability to produce large volumes of coagulation necrosis in a controlled fashion, this technique has gained acceptance as viable therapeutic option for unresectable liver malignancies [1, 3, 31]. Recently, investigation has

been focused on the clinical application of RF ablation in the treatment of lung malignancies [32-36]. Lencioni et al. [37] reported the preliminary results of a multicenter trial in which 106 patients with 186 malignant lung tumors 3.5 cm in diameter or smaller were treated. Diagnoses included NSCLC in 33 patients, metastasis from colorectal cancer in 53, and metastasis from other primary malignancy in 20. Complete ablation of macroscopic tumor as shown by 3-month CT was achieved in 173 of 186 tumors (primary effectiveness rate, 93%). Overall survival was 69% and 49% at 1 and 2 years respectively in patients with NSCLC; 86% and 62% at 1 and 2 years in patients with colorectal cancer metastases. Cancer-specific survival was 91% and 91% at 1 and 2 years in patients with NSCLC; 88% and 72% at 1 and 2 years in patients with colorectal metastases.
A limitation of RF ablation is the relatively small zone of active heating created by ionic agitation (on the order of a few millimetres) [12]. The majority of tissue heating is thus due to thermal conduction, which decreases exponentially away from the source. This results in an inefficient transformation of electrical energy into heat, especially at tissue-vessel interfaces where flowing blood thermally protects perivascular tissue and tumor [38]. Moreover, as temperatures reach 100° C and boiling occurs, increased impedance limits further deposition of electricity into tissue [11]. This becomes even more pronounced if charring occurs; the resultant eschar forms a highly effective insulator around the electrode. A number of different algorithms of energy deposition and several different types of electrodes are used to minimize this effect [39-41].

MW ablation seems to offer many of the advantages of RF ablation while possibly overcoming some of the limitations. MW radiation refers to the region of the electromagnetic spectrum with frequencies from 900 to 2450 MHz. This type of radiation lies between infrared radiation and radio waves. Water molecules are polar; that is, the electric charges on the molecules are not symmetric. The alignment and the charges on the atoms are such that the hydrogen side of the molecule has a positive charge, and the oxygen side has a negative charge [42]. Electromagnetic radiation has electric charge as well; the “wave” representation is

actually the electric charge on the wave as it flips between positive and negative. For a microwave oscillating at 9.2 x 10^8 Hz, the charge changes signs nearly 2 billion times a second (9.2 x 10^8 Hz). When an oscillating electric charge from radiation interacts with a water molecule, it causes the molecule to flip. MW radiation is specially tuned to the natural frequency of water molecules to maximize this interaction. As a result of the radiation hitting the molecules, the electrical charge on the water molecule flips back and forth 2-5 billion times a second depending on the frequency of the MW energy. Temperature is a measure of how fast molecules move in a substance, and the vigorous movement of water molecules raises the temperature of water. Therefore, electromagnetic microwaves heat matter by agitating water molecules in the surrounding tissue, producing friction and heat, thus inducing cellular death via coagulation necrosis [42].

The literature is sparse regarding morphological changes in tissue after MW coagulation therapy, despite a relatively long history of its use since 1979 [43]. It is very important the finding that MW ablation is less affected by the presence of blood vessels than is RF ablation. The majority of tissue heating at RF ablation is caused by thermal conduction, which computer modelling suggests is affected greatly by the heat-sink effect of local blood flow [38]. MW ablation, on the other hand, has a much larger zone of active heating, with the area of active heating being a function of the wavelength of the applied energy [44, 45]. A recent comparative study of RF versus MW ablation in a hepatic porcine model has reported that RF ablation was deflected by 26% in the presence of local blood vessels, while MW ablation was deflected by only 4 % [46].

Certainly, RF can generate larger zones of ablation with cluster electrodes, larger multitined expandable electrodes, or perfusion electrodes. Similarly, MW can create a larger zones of ablation with larger or multiple probes. Recently, a prototype loop-shaped MW antenna was developed that, in animal studies of hepatic tumors, more effectively kills tumors. MW ablation with the loop probes results in complete tumor kill at the ablation/tumor interface, and adjacent to surrounding blood vessels. In addition, vessels within the ablation/tumor interface

failed to show viable cells. The shape of the lesions was not distorted by the proximity to blood vessels. The advantages of this configuration over conventional straight probes include the ability to encircle a tumor, deliver large amounts of precisely targeted MW energy to the tumor, and spare normal liver outside the loop [47].

Several reports regarding MW ablation in the treatment of hepatocellular carcinoma and colorectal metastases, and the showed promising results [48-51].

To our knowledge there are not any clinical trials reported in literature regarding the clinical use of MW ablation in lung tumors. There are few published data from experimental studies, concerning the expected size, quality and pathologic changes of MW ablation in lung tissue. An experimental study in normal canine lung tissue demonstrated that the temperature in lung parenchyma increased to 90-100° C at 5mm from the electrode after 60 sec, and 70-80° C at 10mm after 90 sec at 40 or 60 W. The coagulation area was approximately 20mm in diameter at 40 W and 60 W. The authors concluded the optimal condition in clinical percutaneous MW coagulation therapy to be 40-60 W for 3-4 min of coagulation. Through these parameters, histological findings shortly after MW coagulation showed degeneration and thickening of collagen fiber and exfoliation and ulceration of bronchial epithelium surrounding the electrode [52].

Our study was designed to assess feasibility, safety and effectiveness of MW ablation in an animal model. A comparison with the most widely used image-guided ablative technique, i.e. RF ablation, was also performed. In theory, lung tumors are well suited to MW as well as to RF ablation because the surrounding air in adjacent normal parenchyma provides an insulating effect, thus facilitating energy concentration within the tumor tissue. In fact the dielectric heat energy cannot be generated in the presence of air and selective tumor damage may be achieved, with limited damage to the surrounding normal air-filled lung tissue.

Feasibility and safety of MW ablation are similar to those of RF ablation in our study, performed in a lung rabbit model. Technical success was achieved in 9/10 rabbits in MW ablation group and 9/10 rabbits in RF ablation group. In both cases

technical failure was not due to the ablative procedure but to the anaesthesiology stress in the first case and to pneumothorax after lung puncture in the second case.

One death was encountered in the study. A massive emothorax, depicted at CT scan performed immediately after the procedure, represented the cause of death, that was confirmed at autopsy.

The pneumothorax rate was similar in the two groups of animals, as 4 cases were observed in the MW ablation group and 4 cases were demonstrated in the RF ablation. In one case, in the RF ablation group, drainage was required, while the remaining pneumothoraces and in particular those observed in MW group were all of mild entity and did not require any specific treatment. Also the abscess rate is similar in the two groups (1 per group) and they developed in spite of the antibiotic therapy.

Interestingly, thoracic wall burns were observed in 4 out of 10 animals in MW group. All of them were in the site of needle entry where, during the procedure, the skin was heated up together with the needle shaft and the cable. A possible explanation was given by the retrospective inspection of initial probe positioning at CT images. It revealed that the proximal edge of the exposed tip was probably in contact with the chest wall at the scar site, causing thermal injury to chest wall. Another possible explanation is that the direct heating produced by MW was not sufficiently concentrated at the needle tip. This could be due to the fact that the device is still prototypal and needs to be improved. However at autopsy, no severe damage of organs adjacent to the lungs was observed and major arterial and venous pulmonary vessels were preserved, in the absence of sign of thrombosis or parietal damage. Therefore the heat production and the ablation zone is well demarcated at the tip of the electrode, with no serious risk of damage of important structures located beyond the needle tip.

MW and RF ablation zones were indistinguishable at immediate CT and their mean longest diameter was not significantly different. It has however to be taken into consideration that the exposed tip of the two electrodes were slightly different (1.6 cm for MW and 2 cm for RF electrodes). This could mean a slight increase in

the size of ablation zone produced by MW when compared to RF ablation.

The mean longest diameter of the ablation zones were similar also on gross examination: 12.1mm ± 3.2 and 14.8 mm ± 4.9 respectively for MW and RF ablation. These sizes were however different from those measured at CT, immediately after the procedure. The possible explanations are that at CT we measure both the ablation zone and a peri-ablation area of hemorrhagic suffusion. At 3 and 7 days after the procedure, when the pathological specimens were collected, these phenomenon was decreased and at pathology it is easy to distinguish the necrotic zone from the peripheral hemorrhagic area.

At histopathology, zones of thermal injuries in MW and RF group were similar, with septal necrosis, edema, hemorrhage and peripheral lymphocytic infiltrate. No significant differences at histopathology were demonstrated in ablation zone organization between specimen collected at 3 and 7 days after the procedures. Thrombosis of small vessels surrounding the ablation zone was extensively depicted in MW ablation specimens and focally present in RF ablation specimens. This finding seems to demonstrate the claim that MW ablation is less affected by the presence of small blood vessels than is RF ablation. Improved performance near blood vessels may be caused by the large zone of active heating at MW ablation in comparison to the relative dependence of RF ablation on passive thermal conduction. Alternatively, high temperatures generated at MW ablation may overcome the cooling effect of blood flow. The improved performance of MW ablation near small blood vessels, combined with the ability to use multiple simultaneous probes, could make MW ablation a promising alternative to conventional ablative therapies. If local tumor recurrence is often due to survival of tumor cells near local blood vessels, MW ablation may help reduce recurrence following ablative therapy. The demonstration of the ability of MW ablation to destroy lung tissue located in the proximity of large vessels would greatly expand the indication for clinical use and would enable successful treatment of lesions that are difficult to eradicate by RF ablation.

Assessment of any early/late damage to arterial or venous vessels when

ablating adjacent lung parenchyma is crucial to prevent fatal/major complications in clinical use. A study with a larger animal model would therefore be needed to evaluate the safety and effectiveness of MW ablation in ablating central areas of the lung located in the proximity or adjacent to arterial and venous vessels/airways and to assess the presence/absence/degree of the heat sink effect in MW ablation.

In conclusion, feasibility and safety of MW ablation are similar to those of RF ablation in a lung rabbit model. MW and RF ablation zones are similar in pathologic appearance. MW ablation produces a greater damage to peripheral small vessels inducing thrombosis. Demonstration of the ability of MW ablation to destroy normal lung tissue is clinically relevant, as it would enable creation of a safety margin of ablation of pulmonary parenchyma around lung tumors, which is expected to result in higher rates of complete tumor eradication and lower rates of local recurrence. These findings represent a promising background for future studies investigating the ability and the safety of MW ablation in ablating central areas of the lung located in the proximity or adjacent to arterial and venous vessels/airways. Demonstration of the ability of MW ablation to destroy lung tissue located the proximity of large vessels would greatly expand the indication for clinical use and would enable successful treatment of lesions that are difficult to eradicate by RF ablation. Comparison between the MW and RF ablation will moreover enable development of precise indications/contraindications for each technique in clinical use.

REFERENCES

1. Dodd GD III, Soulen MC, Kane RA, et al (2000) Minimally invasive treatment of malignant hepatic tumors: at the threshold of a major breakthrough. RadioGraphics 20: 9-27
2. Goldberg SN, Gazelle GS, Mueller PR (2000) Thermal ablation therapy for focal malignancies: a unified approach to underlying principles, techniques, and diagnostic imaging guidance. AJR Am J Roentgenol 174: 323-331
3. Lencioni R, Cioni D, Bartolozzi C (2001) Percutaneous radiofrequency thermal ablation of liver malignancies: technique, indications, imaging findings and clinical results. Abdom Imaging 26: 345-360
4. Goldberg SN, Gazelle GS, Compton CC, et al (1995) Radiofrequency tissue ablation in the rabbit lung. Acad Radiol 2: 776-784
5. Goldberg SN, Gazelle GS, Compton CC, et al (1996) Radio-frequency tissue ablation of VX2 tumor nodules in the rabbit lung. Acad Radiol 3: 929-935
6. Dupuy DE, Zagoria RJ, Akerley W, et al (2000) Percutaneous radiofrequency ablation of malignancies in the lung. AJR Am J Roentgenol 174: 57-59
7. Zagoria RJ, Chen MY, Kavanagh PV, et al (2001) Radio-frequency ablation of lung metastases from renal cell carcinoma. J Urol 166: 1827-1828
8. Herrera LJ, Fernando HC, Perry Y, et al (2003) Radiofrequency ablation of pulmonary malignant tumors in nonsurgical candidates. J Thorac Cardiovasc Surg 125:929-937
9. Lencioni R, Fontanini G, Chella A, et al (2002) Percutaneous image-guided radiofrequency thermal ablation of the lung. Eur Radiol 12(Suppl 1): 313
10. Steinke K, Habicht JM, Thomsen S, et al (2003) CT-guided radiofrequency ablation of a pulmonary metastasis followed by surgical resection. Cardiovasc Intervent Radiol 25: 543-546
11. Goldberg SN, Gazelle GS, Solbiati L, et al (1996) Radiofrequency tissue ablation: increased lesion diameter with a perfusion electrode. Acad Radiol 3: 636-644
12. Organ LW (1976) Electrophysiologic principles of radiofrequency lesion making. Appl Neurophysiol 39: 69-76
13. Lu DS, Raman SS, Vodopich DJ, et al (2002) Effect of vessel size on creation of hepatic radiofrequency lesions in pigs: assessment of the "heat sink" effect. AJR Am J Roentgenol 178: 47-51
14. Skinner MG, Iizuka MN, Kolios MC, et al (1998) A theoretical comparison of energy sources – microwave, ultrasound and laser – for interstitial thermal therapy. Phys Med Biol 43: 3535-3547

15. Stauffer PR, Rossetto F, Prakash M, et al (2003) Phantom and animal tissues for modelling the electrical properties of human liver. Int J Hyperthermia 19: 89-101
16. Wright AS, Lee FT Jr, Mahvi DM (2003) Hepatic microwave ablation with multiple antennae results in synergistically larger zones of coagulation necrosis. Ann Surg Oncol 10: 275-283
17. Shock SA, Meredith K, Warner TF, et al (2004) Microwave ablation with loop antenna: in vivo porcine liver model. Radiology 231: 143-149
18. Ginsberg RJ, Vokes EE, Raben A (1997) Cancer of the lung: Non-small cell lung cancer. In: Cancer: Principles and Practice of Oncology, 5th ed. Philadelphia, PA: Lippincott-Raven Publishers; pp 849-857
19. Fry WA, Phillips JL, Menck HR (1999) Ten-year survey of lung cancer treatment and survival in hospitals in the United States: a national cancer data base report. Cancer 86: 1867-1876
20. Birim O, Kappetein AP, Goorden T, van Klaveren RJ, Bogers AJ (2005) Proper treatment selection may improve survival in patients with clinical early-stage nonsmall cell lung cancer. Ann Thorac Surg 80:1021-1026
21. Iwasaki A, Shirakusa T, Enatsu S, Maekawa S, Yoshida Y, Yoshinaga Y (2005) Surgical treatment for lung cancer with COPD based on the Global Initiative for Chronic Obstructive Lung Disease (GOLD). Thorac Cardiovasc Surg 53:162-167
22. Rowell NP, Williams CJ (2001) Radical radiotherapy for stage I/II non-small cell lung cancer in patients not sufficiently fit for or declining surgery (medically inoperable): a systematic review Thorax 56:628-638
23. Rice D, Kim HW, Sabichi A, et al (2003) The risk of second primary tumors after resection of stage I non-small-cell lung cancer Ann Thor Surg 76: 1001-1008
24. Yankelevitz DF, Gupta R, Zhao B, et al (1999) Small pulmonary nodules: evaluation with repeated CT-preliminary experience. Radiology 212: 561-566
25. Lillington GA, Caskey CC (1993) Evaluation and management of solitary and multiple pulmonary nodules. Clin Chest Med 14: 111-119
26. Clegg A, Scott DA, Sidhu M, Hewitson P, Waugh N (2001) A rapid and systematic review of the clinical effectiveness and cost-effectiveness of paclitaxel, docetaxel, gemcitabine and vinorelbine in non-small-cell lung cancer. Health Technol Assess 5:1-195
27. Inoue M, Kotake Y, Nakagawa K, et al (2000) Surgery for pulmonary metastases from colorectal carcinoma. Ann Thorac Surg 70: 380-383
28. Pastorino U, Buyse M, Godehard F, et al. for the International Registry of Lung Metastases (1997) Long-term results of lung metastasectomy: prognostic analysis based on 5206 cases. J Thorac Cardiovasc Surg 113: 37-49

29. Kandolier D, Kromer E, Tuchler H, et al (1998) Long-term results after repeated surgical removal of pulmonary metastases. Ann Thorac Surg 65: 909-912
30. Elias A (1993) Chemotherapy and radiotherapy for regionally advanced non-small-cell lung cancer. Chest 103(Suppl 4): 362-366
31. Vogl TJ, Müller PK, Mack MG, et al (1999) Liver metastases: interventional therapeutic techniques and results, state of the art. Eur Radiol 9: 675-684
32. Sewell PE, Vance RB, Wang YD (2000) Assessing radiofrequency of non-small lung cancer with positron emission tomography (PET). Radiology 217(P): 334
33. Dupuy DE, Mayo-Smith WW, Di Petrillo T, et al (2001) Clinical experience of pulmonary radiofrequency ablation in 27 patients. Radiology 221(P): 389
34. Kang S, Lao R, Liao W, et al (2001) Effect of radiofrequency ablation on lung cancer. ASCO Program/Proceedings 20: 1342
35. King J, Zhao J, Glenn D, et al (2001) Percutaneous imaging-guided radio-frequency ablation of secondary colorectal cancers in lung. ASCO Program/Proceedings 20: 2203
36. de Baere T, Palussiere J, Auperin A, et al (2006) Midterm local efficacy and survival after radiofrequency ablation of lung tumors with minimum follow-up of 1 year: prospective evaluation. Radiology 240: 587-596
37. Lencioni R, Crocetti L, Cioni R, et al (2006) Radiofrequency ablation of pulmonary tumors response evaluation (RAPTURE) trial: final report. European Congress of Radiology (ECR) Annual Meeting 2006
38. Tungjitkusolmun S, Staelin ST, Haemmerich D, et al (2002) Three-dimensional finite element analyses for radio-frequency hepatic tumor ablation. IEEE Trans Biomed Eng 49: 3-9
39. Rossi S, Buscarini E, Garbagnati F, et al (1998) Percutaneous treatment of small hepatic tumors by an expandable RF needle electrode. AJR Am J Roentgenol 170: 1015-1022
40. Goldberg SN, Solbiati L, Hahn PF, et al (1998) Large-volume tissue ablation with radiofrequency by using a clustered, internally cooled electrode technique: laboratory and clinical experience in liver metastases. Radiology 209: 371-379
41. Lee JM, Han JK, Chang JM, et al (2006) Radiofrequency ablation in pig lungs: in vivo comparison of internally cooled, perfusion and multitined expandable electrodes. Br J Radiol 79: 562-572
42. Simon CF, Dupuy DE, Mayo-Smith WW (2005) Microwave ablation: principles and applications. Radiographics 25: S69-S83
43. Tabuse K (1979) A new operative procedure of hepatic surgery using a microwave tissue coagulation. Arch Jpn Chir 48: 160

44. Deardorff DL, Diederich CJ, Nau WH (2001) Control of interstitial thermal coagulation: comparative evaluation of microwave and ultrasound applicators. Med Phys 28: 104-117
45. Liang P, Dong B, Yu X, et al (2001) Computer-aided dynamic simulation of microwave-induced thermal distribution in coagulation of liver cancer. IEEE Trans Biomed Eng 48: 821-829
46. Wright AS, Sampson LA, Waener TF, et al (2005) Radiofrequency versus microwave ablation in a hepatic porcine model. Radiology 236: 132-139
47. Meredith K, Lee F, Henry MB, et al (2005) Microwave ablation of hepatic tumors using dual-loop probes: results of a phase I clinical trial. J Gastrointest Surg 9: 1354-1360
48. Lu MD, Chen JW, Xie XY, et al (2001) Hepatocellular carcinoma: US-guided percutaneous microwave coagulation therapy. Radiology 221: 167-172
49. Abe T, Shinzawa H, Wakabayashi H, et al (2000) Value of laparoscopic microwave coagulation therapy for hepatocellular carcinoma in relation to tumor size and location. Endoscopy 32: 598-603
50. Kato T, Tamura S, Tekin A, et al (2001) Use of microwave coagulation therapy in liver transplant candidates with hepatocellular carcinoma: a preliminary report. Transplant Proc 33: 1469
51. Shibata T, Niinobu T, Ogata N, et al (2000) Microwave coagulation therapy for multiple hepatic metastases from colorectal carcinoma. Cancer 89: 276-284
52. Furukawa K, Miura T, Kato Y, et al (2005) Microwave coagulation therapy in canine peripheral lung tissue. J Surg Res 123: 245-250